Effect of HEMA on protein S-glutathionylation in BEAS-2B cells

Solveig Uvsløkk

November, 2017

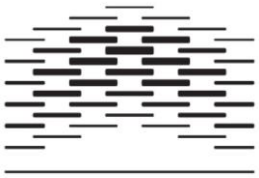

OSLO AND AKERSHUS
UNIVERSITY COLLEGE
OF APPLIED SCIENCES

Effect of HEMA on protein S-glutathionylation in BEAS-2B cells

Solveig Uvsløkk

Master's Degree in Biomedicine
Oslo and Akershus University College of Applied Sciences
Faculty of Health Sciences,
Department of Life Sciences and Health

Thesis submitted for the Master's degree, 60 ECTS

Written at Nordic Institute of Dental Materials (NIOM)

Supervisors:
Ida S. R. Stenhagen
Jan Tore Samuelsen

November, 2017

OSLO AND AKERSHUS UNIVERSITY COLLEGE OF APPLIED SCIENCES

NIOM
Nordic Institute of Dental Materials

Acknowledgement

This master thesis was completed at Nordic Institute of Dental Materials (NIOM), for the Master degree in Biomedicine at Oslo and Akershus University College of Applied Sciences (HIOA). My supervisors were Dr. Philos. Jan Tore Samuelsen and DPhil Ida S. R. Stenhagen.

I would like to thank NIOM, by Jon E. Dahl for giving me the opportunity to undertake my research at such a great laboratory with a good working environment. To all my co-workers at NIOM I would also like to thank you for the support and humoristic lunch- and coffee breaks.

At HIOA I would like to thank Oliwia Witczak and Toril Tefre for giving me the opportunity to do this master thesis part-time.

My two supervisors have been excellent. Both Jan Tore Samuelsen and Ida S. R. Stenhagen have willingly shared all their knowledge regarding this field of work and made this master thesis extremely interesting and fun. Together with a lot of humor they have held my spirit high, despite challenges. Else Morisbak and Bergitte Pearl Olderbø have also been important support and help, thank you.

Last I would like to thank my family and friends for their patience these past 2.5 years. I am returning back into your lives soon. But especially thanks to Carina and Kari Anne. Thank you for making me dance in moments of doubt, saving both me and this master thesis.

You have all been an important contribution to this thesis and to me in general. I am forever grateful.

Oslo, November 2017
Solveig Uvsløkk

Sammendrag

Resin-baserte tannbehandlingsmaterialer er et vanlig førstevalg ved tannbehandling. Både tannhelsepersonell og pasienter eksponeres for metakrylat-monomerer som er en hovedkomponent i disse materialene. På bakgrunn av usikkerhet rundt mulige bivirkninger av disse materialene er det gjennomført en rekke *in vitro* studier. Selv om et cytotoksisk potensial er godt dokumentert *in vitro* er det fortsatt lite detaljert kunnskap om de molekylære interaksjonene mellom monomerer og levende celler. Det er imidlertid foreslått at tiol-reaktivitet og økt nivå av oksidativt stress er underliggende årsaker. Det vist at 2-hydroksyetylmetakrylat (HEMA) kan reagere med tiol-gruppen i glutation (GSH), og det er spekulert om tilsvarende reaksjoner mellom proteiner og HEMA kan skje. Målet med denne oppgaven var å undersøke hvordan den mye benyttede monomeren HEMA kan påvirke cystein i proteiner.

En bronkial epitelial cellelinje (BEAS-2B) ble benyttet som modell i denne *in vitro* studien. Resultatene viste at eksponering for HEMA (4-10 mM) reduserer celleviabiliteten. I tillegg reduserte HEMA nivået av fritt GSH og S-glutationylering av minst ett protein (MW ca. 42 kDa). Disse endringene ble også observert ved konsentrasjoner lavere enn de som påvirket celleviabiliteten. Resultatene tyder videre på at det observerte proteinet er β-aktin. Selv om S-glutationylering av β-aktin antas å kunne påvirke cytoskjelettet ved å hemme polymerisering av aktin, kunne studien ikke påvise endring i aktin-strukturen etter HEMA-eksponering. LC-MS analyser av syntetiske peptiders binding til HEMA antyder at HEMA kan binde S-glutationyleringssetet i β-aktin. I tillegg til en slik konkurrerende binding tyder forsøk med hemming av GSH-syntesen på at cellens GSH-nivå også har betydning for S-glutationylering av β-aktin.

Abstract

Resin-based dental materials are a common first choice when restoring dental function. Both dental personnel and patients are exposed to methacrylate monomers, one main component in these materials. A concern regarding possible side effects these materials may induce has been the motivation of several *in vitro* studies. A cytotoxic potential have been described *in vitro*, but detailed knowledge regarding molecular interactions of monomers in living cells remain scarce. A suggested mechanism, however, involves thiol-reactivity and increased levels of oxidative stress. 2-Hydroxyethylmethacrylate (HEMA) is shown to form spontaneous adduct formation towards the thiol-group in glutathione (GSH), and it is speculated if similar reactions between proteins and HEMA occurs. The aim of this study was to investigate if the commonly used methacrylate HEMA affects protein cysteines.

For this in *vitro study,* a bronchial epithelial cell line (BEAS-2B) was used as a model. Results showed that exposure to HEMA (4-10 mM) reduced the cell viability. In addition, HEMA reduced the level of GSH and S-glutathionylation of at least one protein (MW approx. 42 kDa). These changes were also observed for concentrations lower than those affecting the cell viability. The results further imply that the observed protein is β-actin. Although, S-glutathionylation of β-actin is suggested to affect the cytoskeleton by inhibiting polymerisation of actin, this study could not detect any changes in actin structure after HEMA-exposure. LC-MS analysis of binding between synthetic peptides and HEMA implies that HEMA can bind to S–glutathionylation site in β-actin. In addition to this possible competitive binding, results obtained by inhibiting the GSH-synthesis imply that cellular GSH-level also influence the level of β-actin S-glutathionylation.

Abbreviations

AA	Amino acid
Ab	Antibody
BisGMA	Bisphenol A-diglycidylmethacrylate
BSO	Buthionine sulfoximine
BSA	Bovine serum albumin
DMSO	Dimethyl sulfoxide
FBS	Fetal bovine serum
GDMA	Glycerol dimethacrylate
GSH	Glutathione
HEMA	2-Hydroxyethylmethacrylate
LC-MS	Liquid chromatography–mass spectrometry
mBrB	Monobromobimane
MTT	3-(4,5-Dimethylthiazol-2-yl)-2,5-diphenyl tetrazolium bromide
MW	Molecular weight
NIM-DAPI	4´,6-Diamidino-2-phenylindole-dihyrochloride
PBS	Phosphate buffered saline
PI	Promidium iodide
PSH	Cystein residue in protein
PS-SG	S-Glutathionylated protein
PTM	Post-translational modification
ROS	Reactive oxygen species
SDH	Succinate dehydrogenase
SDS	Sodium dodecyl sulphate
SDS-PAGE	Sodium dodecyl sulphate-polyacrylamide gel electrophoresis
SH	Sulfhydryl
TBS	Tris buffered saline
TEGDMA	Triethylene glycol dimethacrylate
UDMA	Urethane dimethacrylate

Contents

1 Introduction

For a long time, the use of biomaterials to regain human function and health has been found in different fields of medicine, including dentistry (1). Any material can be defined as a biomaterial if it is used to make a device to replace a part or a function of the body. Examples of biomaterial devices are contact lenses, catheters, bone implants, tooth fillings and sutures. Regarding biomaterials, it is important to understand the underlying mechanism that defines the material in an acceptable manner of safety, economy, reliability and physiology. Biomaterials commonly interact with living tissue and therefore the biocompatibility of the material is important. Biocompatibility is a wide term and includes how the device is accepted in the tissue, pharmacological acceptability (non-toxic, non-allergic, non-immunogenic) and stability (no time-dependent degradation) (2).

1.1 Dental biomaterials

The materials used to restore function of dental health in humans have varied over the years as the development of different materials and methods has become available. In the early 20th century, the use of amalgam was the leading way of treatment. Both aesthetic considerations and growing awareness of how hazardous mercury is to the environment and human health, has led to amalgam being replaced by resin-based alternatives (figure 1-1) (3, 4). Many countries have implemented a restricted use or ban of amalgam (4). In Norway, a ban of the use of all mercury-containing products, including dental amalgam, was enforced in 2008 (5).

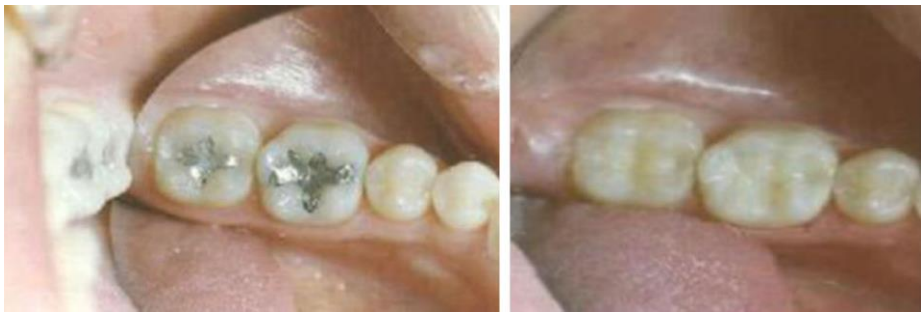

Figure 1-1: Amalgam fillings (left) are often replaced by resin-based dental restorations (right). ©Photo by Jon E. Dahl 2002

1.1.1 Resin-based dental materials

Adhesives, resin-modified glass ionomer cements, resin-based filling materials and fissure sealant agents are examples of resin-based materials routinely used in dentistry (6, 7). These materials are complex, but the common feature is a resin matrix, which consists of methacrylate monomers. Commonly used methacrylates are: bisphenol A-diglycidylmethacrylate (BisGMA), thriethylene glycol dimethylacrylate (TEGDMA), urethane dimethacrylate (UDMA) and 2-hydroxyethylmethacrylate (HEMA) (figure 1-2) (7).

A mixture of methacrylate monomers is used in resin-based restoratives to achieve a material with specific properties. In resin-based filling materials, viscous monomers are used to strengthen the resin matrix in addition to monomers with lower viscosity to enable more filler particles to be added. Filler particles and difuctional monomers are used to decrease shrinkage and increase hardness of the material (7, 8). For the resin-based filling materials to adhere to the enamel or dentin surface of the tooth, an adhesive is placed between the composite and the surface of the dentin (9). In adhesives, monomers with hydrophilic properties are chosen, and the most commonly used is HEMA together with other water soluble methacrylates(9-11). In glass ionomer cement, HEMA is important as a co-solvent to avoid phase separation of the resin from the glass-ionomer components (12). HEMA is also a common component in adhesives used to attach brackets to tooth surfaces in orthodontic treatment, where the patient group usually includes children and youths (13, 14).

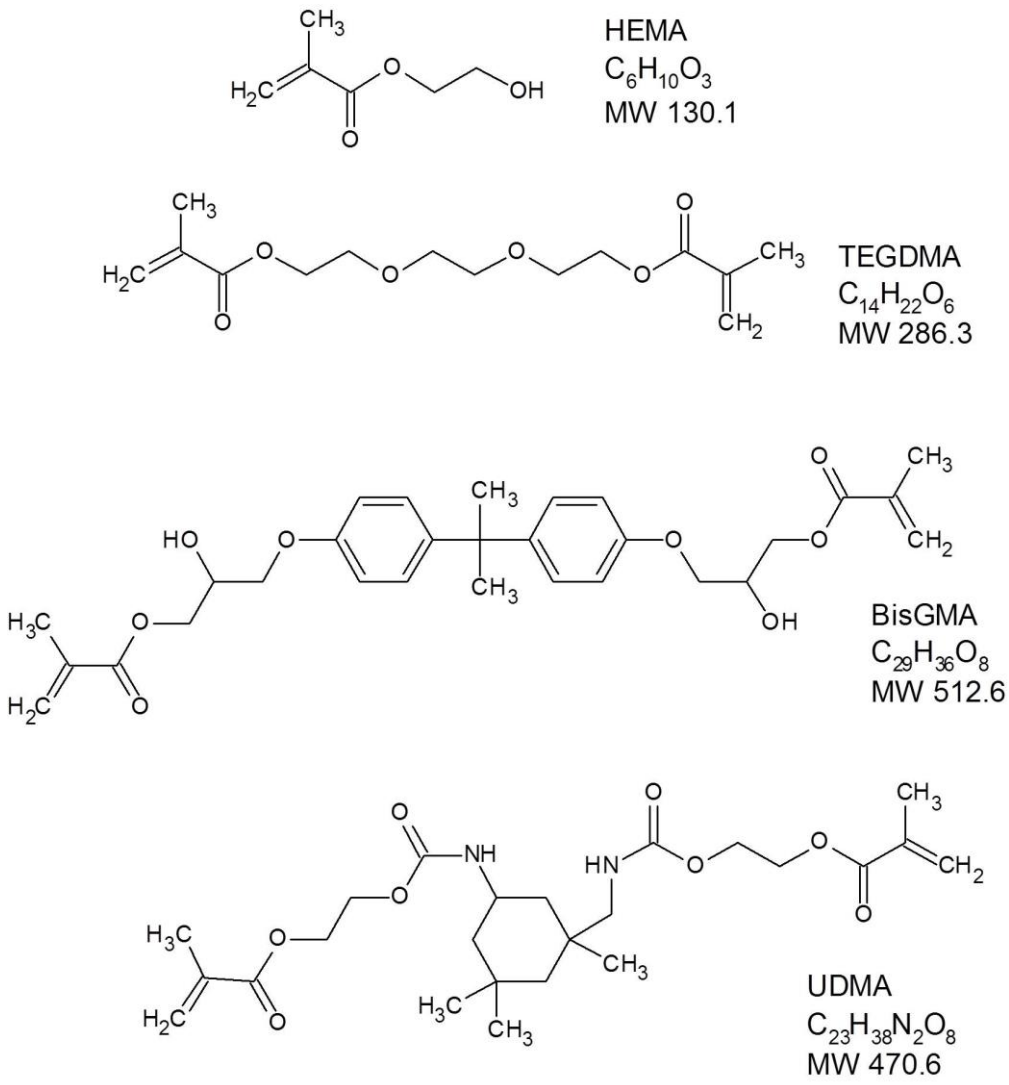

Figure 1-2: Chemical structure, name and molecular weight (MW) of some methacrylates used in resin-based dental materials.

Some methacrylates used in resin-based dental materials are shown in figure 1-2. They vary in the chemical structure and have different properties, but they also have structural similarities. They all have a carboxyl ester group that conjugates with a double bond between the α- and β-carbon. This gives methacrylates the ability to undergo a Micheal-type addition to nucleophiles (15, 16).

The methacrylate monomers in resin-based materials are cured by polymerisation. Many different polymerisation-promoting systems have been developed, but most common is the light curing system (17). A light source of 468 nm is used to excite initiators that start a free radical reaction (8). A free radical is a compound with a reactive unpaired electron that collides with a carbon double bond found in the methacrylate monomers. The free radical pairs with one of the electrons in the double bond, leaving the other electron to become a free radical to react with a new monomer. This reaction continues and the monomers become a polymer chain molecule (figure 1-3) (8). The polymerisation efficiency is measured as degree of conversion (% double bond conversion) and rarely exceeds 70% (18, 19).

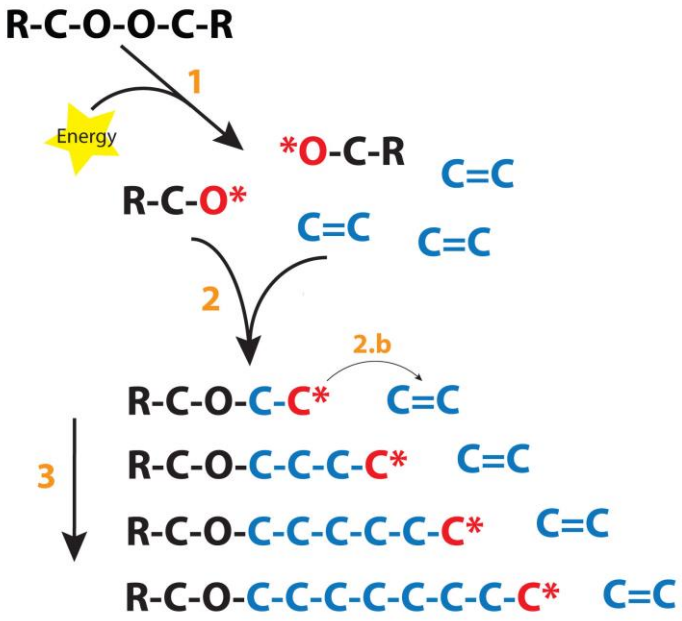

Figure 1-3: Figure showing polymerisation of monomers. (1) An initiator is activated and produces a free radical (R-C-O*). (2) A free radical reacts with carbon double bond (C=C) in monomers. (2.b) A new free radical is produced and reacts with a new monomer (3) and a free radical reaction continues and creates a polymer chain molecule.

1.2 Exposure to methacrylate monomers

Due to incomplete polymerisation, monomers leak after curing and patients are exposed (6, 20, 21). Several research groups have postulated how the chemical substances released from resin-based dental materials are taken up in the human body. This occurs mainly by three routes: through ingestion of released compounds in the gastro-intestinal tract, through diffusion to the pulp through the dentinal tubules, and through uptake of volatile components in the lungs (6, 22-25). In addition, dental personnel are exposed to these monomers on a daily basis while handling uncured materials. The main exposure routes for dental personnel are direct skin contact and airway exposure (26-28). There is a growing concern regarding the toxicity these materials may induce in contact with living organisms(6). However, the knowledge regarding detailed molecular interactions is scarce.

1.3 Toxicity of methacrylate monomers

Current knowledge regarding methacrylate toxicity has mainly been obtained from cell culture studies. HEMA has been studied in different cell culture systems and is shown to induce DNA-damage, cell cycle arrest and cell death (29-32). A suggested underlying mechanism includes observed glutathione (GSH) depletion caused by spontaneous adduct formation between HEMA and cysteine of GSH (16, 33). The reduced GSH levels lead to increased cellular levels of oxidative stress (33, 34). Since HEMA has the ability to form an adduct with cysteine in GSH spontaneously, it is proposed that similar reactions can occur with cysteine residues in proteins (33). Other studies have hypothesized that HEMA has the ability to react with lysine in proteins, which indicates HEMA has the ability to bind towards different complex molecules (35). The role of adduct formation between methacrylate monomers and nucleophilic sites is suggested to be of importance in understanding the mechanisms for the cytotoxic potential of methacrylate monomers (33, 36). This gives reason to investigate the underlying mechanisms of methacrylates and to gather more knowledge on the effects the use of resin-based dental restorative materials has on exposed individuals (37).

1.4 Glutathione

GSH, the tripeptide γ -L-glutamyl-L-cysteinyl-glycine (figure 1-4), is a low-molecular-mass thiol endogenous to mammalian cells and participates in numerous biochemical processes such as redox homeostasis, phase II biotransformation and S-glutathionylation (38). Concentration of GSH in cells varies depending on the cell type, but usually range from 1-10 mM where the majority, around 90%, is found in the cytosol (39-41).

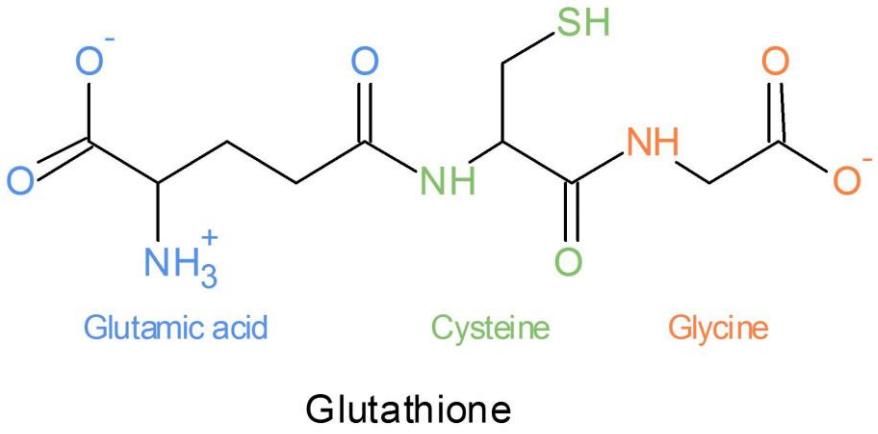

Figure 1-4: Structure of glutathione (GSH) showing the three amino acids; glutamic acid, cysteine and glycine, with a γ-linkage between the N-terminal glutamic acid and cysteine.

As an antioxidant, GSH is important in the protection against cellular oxidative stress (42, 43), an imbalance between oxidants and antioxidants in the favor of the oxidants (44). Glutathione can exist in both reduced (GSH) and oxidized (GSSG; glutathione disulphide) form (39, 40). In response to increased oxidative burden, a disulphide-linkage between two GSH molecules is formed (40). GSSG can, with the help of glutathione-reductase, be reduced back to GSH (45). GSH also serves as an important part of phase II biotransformation. Facilitated by glutathione S-transferase (GSTs), GSH conjugates with substances foreign to the body (xenobiotics) (46). As a rule, binding of GSH decreases the reactivity and increases the water solubility of the foreign substances, thereby promoting their elimination from the body (46, 47).

1.5 S-glutathionylation of proteins

Translation is the process which synthesises proteins based on mRNA sequences. During and after translation, proteins can be modified by post-translational modification (PTM). In general terms, PTM is the modification of amino acid (AA) side chains in the final synthesised protein. Simple or complex chemical groups are attached to the AA residues and structure of the protein is modified and may yield several properties (48). An important PTM in cells is phosphorylation. This is a modification of serine, threonine and tyrosine residues by the addition of phosphate (PO_4^{3-}) (49).

Protein S-glutathionylation is the reversible redox modification of cysteinyl residues in proteins by mixed disulphide bond formation with the thiol-group of GSH (figure 1-5) (38, 50, 51). This modification is also known as S-glutathiolation, protein mixed disulphides or simply glutathionylation (52).

Figure 1-5: Protein S-glutathionylation, where glutathione (GSH) binds towards cysteine residue in protein (PSH) and creates an S-glutathionylated protein (PS-SG)

S-Glutathionylation has not been as widely investigated as many other PTMs. Hence, the knowledge of which roles or effects glutathionylation has on the cell is limited. S-Glutathionylation has been considered to be a part of the cell's reaction during oxidative stress, but this modification has also been observed under basal physiological conditions. As a result, it has been given more attention as significant in general cell regulations (50, 51, 53). S-Glutathionylation has been found to be involved with many cellular processes; control of gene expression, cell proliferation, apoptosis, protection of proteins against oxidative stress and oxidative signal transduction (45, 51, 54).

S-glutathionylation of proteins can be enzymatic or non-enzymatic. Non-enzymatic S-glutathionylation happens mostly during oxidative stress, where the formation of reactive oxygen spices (ROS) is elevated (55). S-Glutathionylation is a reversible modification and is mostly regulated enzymatically by glutaredoxin (Grx), a family of enzymes involved in deglutathionylation of proteins (56, 57). Even though the mechanisms of glutathionylation and deglutathionylation are established, the specific

cellular mechanisms responsible for the formation of S-glutathionylated proteins are mostly unknown(51). The group of identified proteins that are subject to glutathionylation is described as the glutathionome (58). Compared to the proteome the number of proteins in the glutahionome is not large, but new target proteins appear in the literature regularly. One protein reported to be highly S-glutathionylated is actin, found in the cytoskeleton of cells (59-61).

1.6 The cytoskeleton

The cytoskeleton has mainly three functions in the cell. It organizes the content of the cell, connects the internal environment physically and biochemically to the external environment and helps the cell to move and change shape (62). All these are polymer-based mechanisms that together control the mechanics and shape of the cell. As Fletcher et.al describes it; "*The proteins that makes up the cytoskeleton have many similarities to the LEGO, the popular children's toy. Both consists of many copies of a few key pieces that fit together to form larger objects…And both can disassemble and reassembled into different shapes according to changing needs.*"(62)(p.486-487).

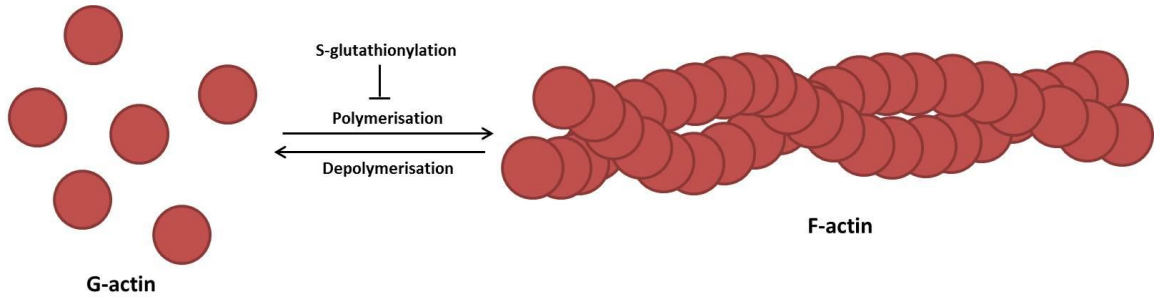

Figure 1-6: Illustration of polymerisation of granular actin (G-actin) to filament actin (F-actin), and depolymerisation from F-actin to G-actin. Polymerisation is inhibited by S-glutathionylation of cysteine residues in F-actin.

The cytoskeleton is divided into three main components: actin filaments, microtubules and intermediate filaments. Actin filaments are found in mammalian cells (59). This part of the cytoskeleton consists of long filament structures built up of granular actin (G-actin) that forms filament actin (F-actin) upon polymerisation (figure 1-6). F-actin are long filament structures found throughout the cell (figure 1-7) (63). There are many regulatory mechanisms where actin can be a subject of modification. These are, amongst

others; acetylation, ADP-ribosylation, arginylation, phosphorylation, and different redox-related modifications (60). One of these modifications, categorised as a redox-related modification, is S-glutathionylation and is reported to affect the polymerisation of actin (51, 64).

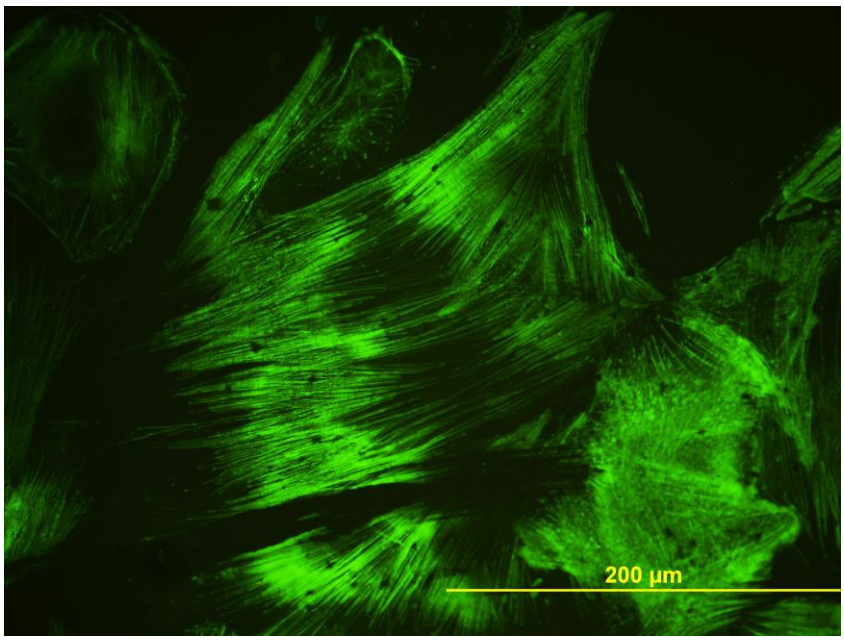

Figure 1-7: F-actin (green) in primary alveolar type II cells from rat lungs, stained with Alexa fluor®488 conjugated Phalloidin. ©Photo by Jan Tore Samuelsen 2010

In the absence of oxidative stress, it is reported that actin is constitutively S-glutathionylated in cells (65). Cys374 in β-actin is the residue most susceptible to S-glutathionylation (60, 66). S-glutathionylation of β-actin does not induce depolymerisation of F-actin, but rather partially inhibits actin polymerisation (61, 64, 67). In this way, S-glutathionylation regulates the polymerisation of actin and thereby the actin dynamics and mechanics, which is essential for cell mobility and organisation (66, 68, 69).

2 Aim

In this study, we hypothesized that cysteine reactivity towards HEMA affects thiol-dependent processes in addition to the described GSH-HEMA adduct formation.

The specific aim of this study was to investigate if HEMA affects protein S-glutathionylation in BEAS-2B cells. Two potential mechanisms of action will be investigated:

A. GSH depletion may influence the amount of protein S-glutathionylation
B. Competitive binding to cysteine sites may block protein S-glutathionylation sites

Both mechanisms will shift the equilibrium towards less S-glutathionylated protein.

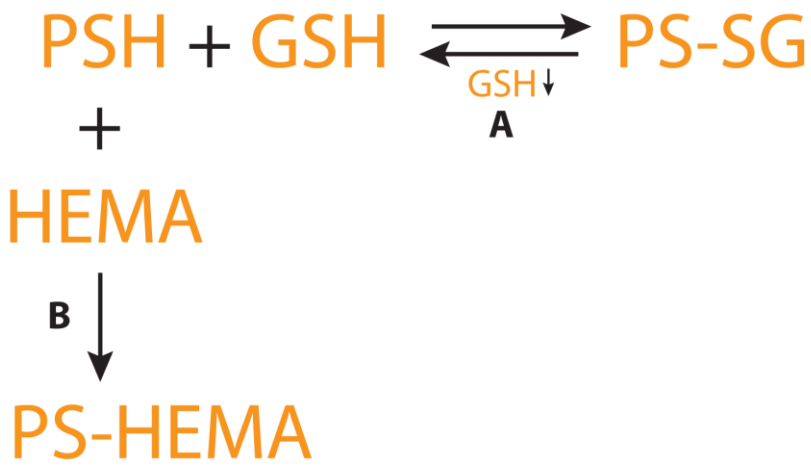

Figure 2-1: Illustration of suggested effects of HEMA exposure on protein S-glutathionylation. (A) GSH depletion may shift the equilibrium to left. (B) HEMA may bind to and block S-glutathionylation sites in proteins.

3 Material and methods

Methods and procedures used in this thesis are described below. For detailed information about reagents, chemicals, equipment and software mentioned, see appendix (chapter 9).

3.1 Cell culturing and cell treatment

3.1.1 BEAS-2B cell line

The cell-line used in this study, BEAS-2B, is a human bronchial epithelial cell line obtained from autopsies of non-cancerous individuals (figure 3-1). Subsequently, the cells have been transformed with Adenovirus 12-SV40. BEAS-2B cells are therefore safety level 2 classified. This gives the cells an extended culture lifespan compared to normal human bronchial epithelial cells (70). The cells were purchased from European Tissue Type Culture Collection (ECACC; Sigma-Aldrich).

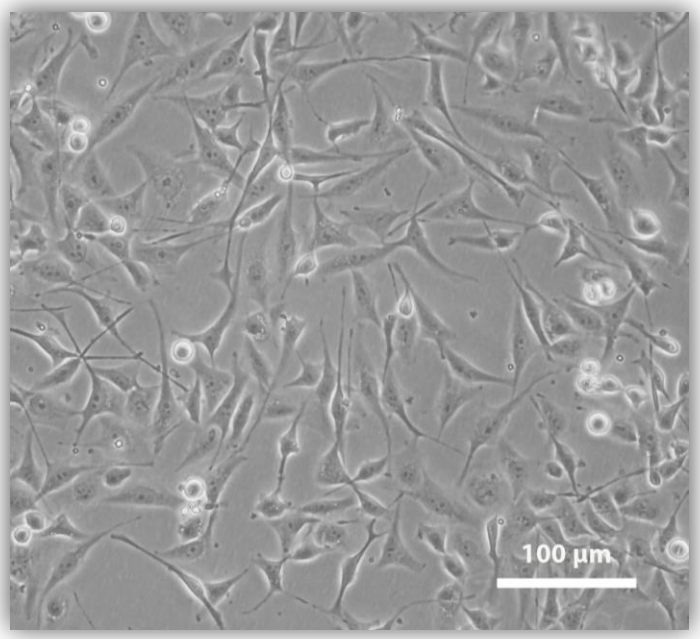

Figure 3-1: Phase-contrast microscopy image of BEAS-2B cells.

3.1.2 Cell culturing

The cells were monitored daily by phase-contrast microscopy. BEAS-2B cells are adherent and were grown in 75 cm^2 cell culture flasks coated with collagen (plate coating protocol see table 9-3). The cells were grown in serum-free media, Lecher and LaVeck (LHC-9 medium; Invitrogen-Life Technologies, CA, USA) and split three times a

week (Monday, Wednesday and Friday) with a density of 30 000 cells/cm^2. The proteolytic enzyme trypsin (0.5 mg/mL; Lonza, Verviers, Belgia) was used to detach cells from the coated surface. Cells were incubated in 37˚C, 5 % CO_2 and 95% relative humidity.

Depending on the method, the cells were cultured in 12- or 24-well plates or in 21 cm^2 dishes coated with collagen, at a density of 30 000 cells/cm^2. They were grown for 24 hours before further exposure and treatment (see table 3-1). In this study, cells were exposed to HEMA (Fluka Chemie AG, Switzerland) and buthionine sulfoximine (BSO; an inhibitor of the rate-limiting step of GSH synthesis (71)) (Sigma-Aldrich, St.Louis, USA).

An aseptic method was used during all treatments of cells. This included working in a Laminar flow cabinet (LAF-bench) with a HEPA filter and all working surfaces and equipment were sprayed with a 75% ethanol-based solution prior to use. All disposal of equipment and solutions containing BEAS-2B cells were autoclaved (134˚C, 60 minutes) or disinfected with 2% vircon (DuPont Comp., Suffolk, USA) according to guidelines from European Union Council Directive 98/24/EC April 7th 1998, for biological material classified with safety level 2 (72).

Table 3-1: Exposure conditions for BEAS-2B cell cultures for the different methods used in this study.

Method	Exposure	Exposure time (hours)
Cell viability assay, MTT	0.5, 1, 2, 4, 6, 8, 10 mM HEMA 5, 10, 25, 50, 100 µM BSO	24 h 24 h
Cell death	0.5, 1, 2, 4, 6, 8, 10 mM HEMA	24 h
Cell cycle analysis	0.5, 1, 2, 4, 6, 8, 10 mM HEMA 10, 50, 100 µM BSO	24 h 24 h
Glutathione measurement	0.5, 1, 2, 4, 6, 8, 10 mM HEMA 10, 50, 100 µM BSO	4, 8 h 4, 8 h
Immunofluorescence	2 mM HEMA	6 h
Western blot	2 mM HEMA 10, 50, 100 µM BSO	4,6,8 h 6,8 h

3.2 Spectrophotometry - Cell viability assay, MTT

The MTT-assay is a viability test where the activity of a mitochondrial enzyme, succinate dehydrogenase (SDH), is measured by spectrophotometry (73, 74). The method is well established and used in standardisation for testing the toxicity of materials *in vitro* (75).

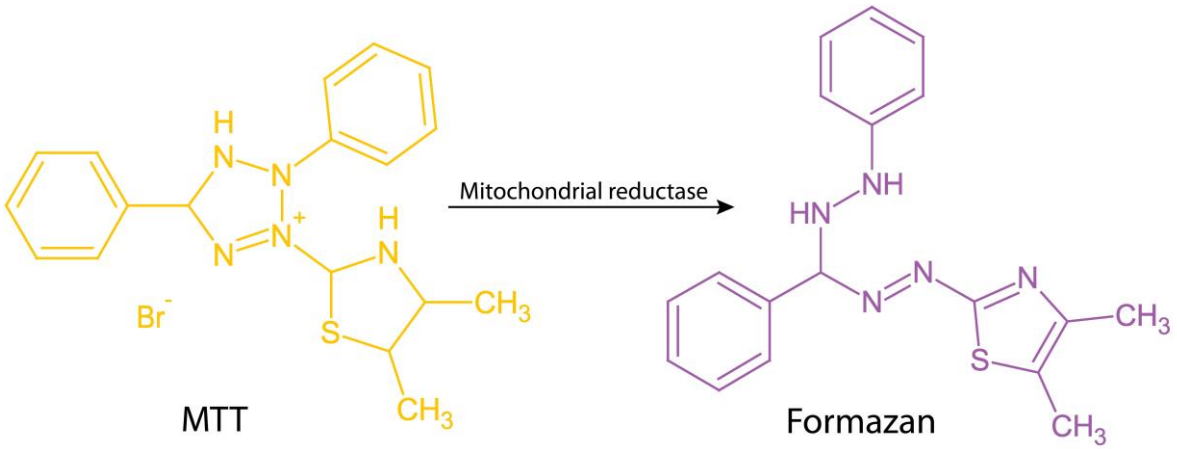

Figure 3-2: Illustration of reduction of 3-(4,5-dimethylthiazol-2-yl)-2,5-diphenyl tetrazolium bromide (MTT) to formazan.

The reagent 3-(4,5-dimethylthiazol-2-yl)-2,5-diphenyl tetrazolium bromide (MTT) is taken up by the mitochondria in cells where SDH transforms MTT to formazan (figure 3-2). The colour of the MTT-reagent is yellow but changes colour to purple when reduced to formazan. Dimethyl sulfoxide (DMSO) is used to dissolve the formazan and then be measured by spectrophotometry.

Procedure

1. After end of exposure remove medium in each well
2. Add 400 µL MTT-solution (0.5 mg/mL) to each well
3. Incubate at 37˚C for 1 hour
4. Remove the supernatant and add 400 µL DMSO to each well
5. Incubate at room temperature for 20 minutes
6. Measure absorbance of each well on a multiwell scanning spectrophotometer at a wavelength of 570 nm

3.3 Fluorescence microscopy – cell death determination

To count viable, necrotic and apoptotic cells, the cells were stained with a fluorescent staining solution containing propidium iodide (PI) and Hoechst 33342. Depending on whether the cell membrane is intact or not, the cells are stained differently. PI stains DNA in cells where the membrane is not intact, and are characterised as necrotic cells (non-programmed cell death). Necrotic cells can be seen as red in the microscope. Hoechst stains DNA in all cells. Both viable and apoptotic cells will be seen as blue in the microscope, but the DNA is condensed in apoptotic cells and can be seen with more intense staining (figure 3-3).

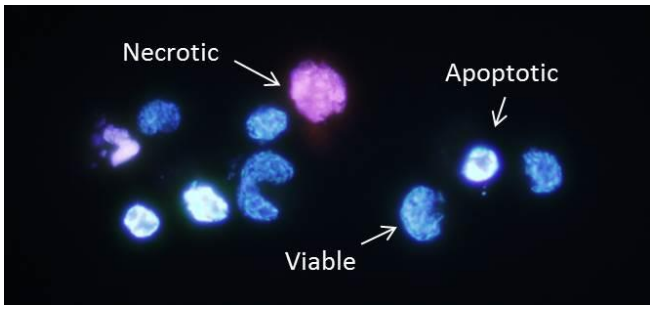

Figure 3-3: Picture of cells stained with propidium iodide and Hoechst 33342 for categorization of necrotic, apoptotic and viable cells.

Procedure

1. After end of exposure transfer medium in each well to a 1.5 mL tube
2. Wash each well once with PBS
3. Add 100 µL trypsin to each well
4. Incubate at 37˚C for 2-3 minutes
5. Transfer supernatant to the tube containing the respectively medium
6. Centrifuge (50 x g, 4˚C, 5 minutes) tubes
7. Add 50 µL FBS with Hoechst 33342 (10 µg/µL) and PI (10 µg/µL) to each tube
8. Incubate at room temperature for 30 minutes, light protected
9. Add 1 mL of PBS to each tube
10. Centrifuge (50 x g, 4˚C, 5 minutes) tubes and remove supernatant
11. Add 50 µL of FBS to each tube
12. Add one drop to a slide, spread it out and leave to dry while light protected
13. Count 300 cells of each sample and categorise as viable, necrotic or apoptotic using a fluorescence microscope with the excitation filter 345-355 nm

3.4 Flow cytometry - Cell cycle analysis

Before a cell moves into mitosis (M-phase) and divides, it progresses through stages of a cell cycle. These stages are gap 1 (G1) phase, synthesis (S) phase and gap 2 (G2) phase (figure 3-4). Throughout the cell cycle, there are checkpoints where the cell is checked for flaws in the genome or the rest of the cell. When an error is detected the cell cycle progression is halted and does not progress until it is resolved. In the case of a non-repairable damage the cell may activate apoptosis. If no error is detected, the cell goes through every phase and into mitosis and divides (49).

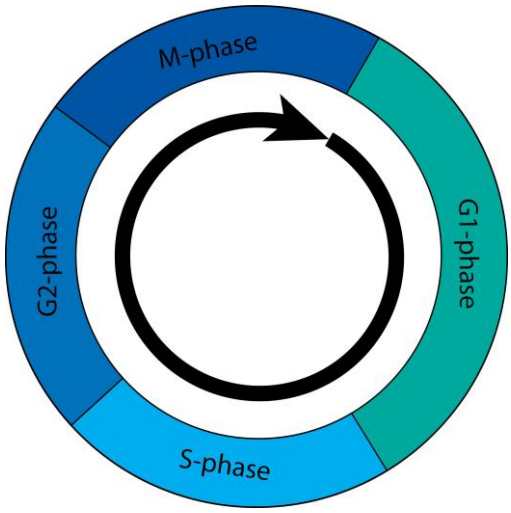

Figure 3-4: Illustration of cells progression through different phases in a cell cycle.

Since the DNA duplicates during a cell cycle, it is possible to determine which phase a cell is in by measuring the amount of DNA present in the cell. DNA can be stained with fluorescent markers and analysed using flow cytometry. Flow cytometry is a method where light scattering and fluorescence intensity are measured for each individual cell in a single cell suspension. The reagent used in this method is nuclear isolation medium containing 4´,6-diamidino-2-phenylindole dihydrochloride (NIM-DAPI). The solution intercalates AT-rich areas in DNA. Intensity of fluorescence measured, is directly proportional to the amount of DNA in the cell.

Procedure

1. After end of exposure remove medium in each well
2. Wash each well with PBS
3. Add 100 µL trypsin to each well
4. Incubate at 37˚C for 2-3 minutes
5. Add 500 µL PBS with 5% FBS to each well and transfer to 1.5 mL tubes
6. Centrifuge (50 x g, 4°C, 5 minutes) tubes
7. Add 150 µL Citrate buffer to each tube
8. Add 300 µL Staining-solution (NIM-DAPI) to each sample
9. Incubate at room temperature for 15 minutes, light protected
10. Measure fluorescence intensity of each sample using a flow cytometer
11. Analyse data with Multicycle software

3.5 Flow cytometry – Glutathione measurement

As mentioned in the previous section, flow cytometry can be used to determine the contents in each cell in a single cell suspension if the cells are stained with fluorescent markers. Fluorescence of monobromobimane (mBrB) depends on the binding to sulfhydryl groups (figure 1-4). The fluorescence intensity can be used as a measure of the amount of GSH in the cell (76).

Procedure

1. After end of exposure remove medium from each well
2. Wash each well with PBS
3. Add 100 µL trypsin to each well
4. Incubate at 37˚C for 2-3 minutes
5. Add 400 µL of PBS with FBS (10 µL/mL) and mBrB (1 µL/mL) to each well and transfer to 1.5 mL tubes
6. Incubate on ice for 15 minutes, light protected
7. Measure fluorescence intensity of each sample using a flow cytometer

3.7 SDS-PAGE and Western blotting

Sodium dodecyl sulphate-polyacrylamide gel electrophoresis (SDS-PAGE) and western blot are techniques used to quantify specific proteins in a cell suspension. Together it contains three steps; separation of proteins by size (SDS-PAGE) (figure 3-5), transfer of proteins to a solid phase, and then labelling with specific antibodies (Ab) that can be visualised (western blotting). The proteins are separated in a gel with narrow pores. An electrical field makes the charged proteins able to migrate through the pores in the gel. Smaller proteins migrate faster than larger proteins and the proteins will thereby be separated by size. A marker with molecules of known size is applied next to the samples for comparison. After the separation, the proteins are transferred to a solid phase with yet another electrical field. The negatively charged proteins will travel to the positive end and be trapped in a membrane of nitrocellulose. This solid phase can be incubated with specific Ab towards a protein of interest, and later be measured and analysed (77).

Figure 3-5: Picture of SDS-PAGE equipment.

Procedure – Sample preparation

1. After end of exposure remove medium in each dish
2. Wash each dish with PBS
3. Add 200 µL sample buffer
4. Use a cell scraper to detach cells from the bottom of the dish and transfer sample to 1,5 mL tubes
5. Incubate at room temperature overnight
6. Sonicate samples and add 5% 2-mercapotoethanol or dH_20, depending on the desire to reduce disulphide bonds in the proteins
7. Store samples at -20 °C until usage

Procedure – SDS-PAGE and western blot

1. Prepare 10% SDS-PAGE gels according to table 9-5 with the Mini-PROTEAN® Tetra handcast systems from Bio-Rad
2. Add 2 µL molecular weight marker and 12 µL of each sample to wells
3. Separate proteins with electrophoresis before blotting onto a nitrocellulose membrane overnight
4. After blotting stain the membrane with Poncau to visually investigate transfer of proteins
5. Block the membrane using 5% milk (or 5% BSA) in TBS-T at room temperature for 30 minutes
6. Dilute primary Ab in TBS-T with 1% milk (or 1% BSA) and add to the membrane
7. Incubate at 4˚C overnight
8. Wash the membrane in TBS-T at room temperature for 10 minutes, three times
9. Dilute secondary Ab in TBS-T with 1% milk (or 1% BSA) and add to the membrane
10. Incubate at room temperature for 2 hours, light protected
11. Wash membrane in TBS-T at room temperature for 10 minutes, three times
12. Air-dry the membrane, light protected
13. Scan the membrane with Odyssey CLx Scanner and analyse data in Image Studio software version 5.2

3.6 Fluorescence microscopy – Immunofluorescence

Using specific Ab marked with fluorochromes, proteins and other targets in cells can be stained and studied with fluorescence microscopy. This method is used to observe possible changes in protein expression or location of the targets in cells exposed for different treatments. Cells have to be fixed so they are permeable for staining with the specific Ab. Depending on the target of interest; the cells can be fixed either with methanol or paraformaldehyde. When fixed with paraformaldehyde, the cells need to be permeabilised with a detergent.

Procedure

1. After end of exposure remove medium in each dish
2. Cover cells in 2-3 mm with 4% paraformaldehyde
3. Incubate at room temperature for 10 minutes
4. Wash each dish in PBS for 5 minutes, three times
5. Cover each dish in PBS, with 0.3% Triton x100 and 5% BSA, in room temperature for 60 minutes
   (For direct Alexa fluor® conjugated phalloidin proceed directly to step 8)
6. Remove solution, dilute primary Ab in PBS with 0.3%Triton x-100 and 1% BSA and add to each dish
7. Incubate at 4°C, overnight
8. Wash each dish in PBS for 5 minutes, three times
9. Dilute secondary Ab in PBS with 0.3%Triton x-100 and 1% BSA and add to each dish
10. Incubate at room temperature for 2 hours (15 minutes for Alexa fluor ® conjugated phalloidin)
11. Wash each dish in PBS for 5 minutes, three times
12. Apply Prolong® Gold Antifade Reagent with DAPI and mount with coverslip

3.8 Liquid chromatography–mass spectrometry (LC-MS)

In this study, ultra-high performance liquid chromatography (UHPLC)-mass spectrometry (MS) was used to investigate the adduct formation between different synthetic peptides and HEMA (figure 3-6). Liquid chromatography is a method where a complex sample is resolved and separated into its individual components. This is achieved by eluting the sample through a column (stationary phase) using a liquid (mobile phase). The components elute at different times from the stationary phase based on their polarity and structural characteristics. After elution, components pass into the ion source of the MS-instrument. MS is a technique where ions are separated according to mass-to-charge (m/z) ratio (figure 3-7) (78).

Figure 3-6: Picture of the UHPLC-MS used in this study. ©Photo Agilent Technologies, CA, USA

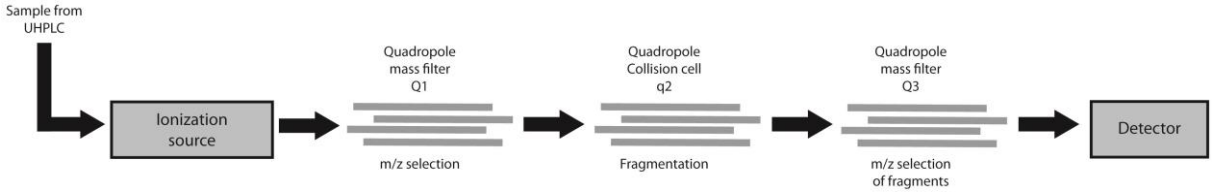

Figure 3-7: Principles of QqQ-MS. Sample from UHPLC is ionized before entering the first quadrupole (Q1) for first m/z selection. In the collision cell (q2), the selected ions are fragmented before the second m/z selection (Q3) and finally detected.

3.8.1 Instrument specifications

For the peptide analyses, a 1290 II Infinity UHPLC connected to a 6470 triple quadrupole (QqQ) MS from Agilent was used. Chromatographic separation was achieved using a Zorbax RBHD bonus-RP C18 (2.1 x 50mm, 1.8µm) column. The mobile phase was distilled H_2O (0.1% formic acid) and acetonitrile and a gradient was used. The samples were ionized using electrospray ionization (ESI) and data was acquired in MS2 scan mode (m/z: 100-1000). Mass spectra of the peptides were compared to those reported by the manufacturer.

3.8.2 Peptides

Synthetic peptides were ordered from GenScript, USA. All peptides were based on the last 14 amino acids of the carboxyl-terminus of β-actin. Peptides with or without the nucleophilic AA cysteine and lysine were chosen (Table 3-2).

Table 3-2: Amino acid (AA) sequence of synthetic peptides ordered from GenScript, USA.

Name	Sequence	Number AA	Theoretical MW (g/mol)*
Synthetic peptide	YDESGPSIVHRKCF	14	1637.7
Synthetic peptide without cysteine (C)	YDESGPSIVHRK-F	13	1534.8
Synthetic peptide without lysine (K)	YDESGPSIVHR-CF	13	1509.5
Synthetic peptide without C and K	YDESGPSIVHR--F	12	1406.1

* Measured by GenScript

3.8.3 Sample Preparation

Each peptide was dissolved in 10 mM ammonium acetate (AMAC) to give a final concentration of 1.3 mg/mL. An interval of different pH values was measured for each peptide sample, four values between pH 5-9 were chosen. To each sample with different pH, 0 or 2mM HEMA was added and incubated overnight at 37˚C. Samples were diluted 1/400 in a mixture of 5% acetonitrile, 0.2% formic acid in H_2O and analysed on UHPLC-MS.

3.9 Statistical analysis

Three or more datasets were performed for statistical analysis. The data obtained from MTT-assay, GSH-measurements and western blotting are all relative values. Therefore, each value was normalized against the sum of all values in the data set to take variations into consideration. The graphs were made and statistical analysis performed in GraphPad Prism 7. One-way ANOVA with Dunnett's or Tukey's multiple comparisons post-test was used. A value of $p<0.05$ was considered statistically significant and marked with "*" in the graphs. Data presented in graphs are shown as mean ± standard deviation (SD).

3.10 Graphs, figures and images

The graphs representing the results in this thesis were made in Graphpad Prism 7. Figures illustrated in this thesis were made by using different software, such as ACD ChemSketch, Adobe Illustrator CS5 and Adobe Photoshop CS5. Fluorescence images were merged by using Adobe Photoshop CS5.

4 Results

4.1 Cell viability

Cellular SDH activity was used as a measure of cell viability. BEAS-2B cells were exposed to different concentrations of HEMA and BSO for 24 hours before SDH activity was measured. Control contained non-exposed cells.

4.1.1 Effects of HEMA on cell viability

Cells exposed to 0.5-2 mM HEMA showed no significant change in viability when compared to control. There was a significant decrease compared to control for cells exposed to 4-10 mM HEMA (figure 4-1). Visual inspection of the cell cultures also indicated a pattern of decreased cell density with increasing HEMA concentrations (figure 4-2).

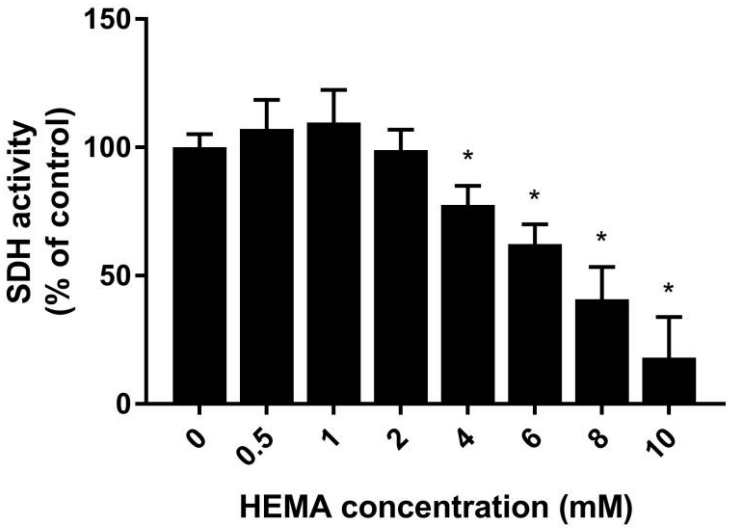

Figure 4-1: Cell viability determined as SDH activity in BEAS-2B cells after 24 hours exposure to HEMA. Results are shown as percentage of control (mean ± SD, n=4). Asterisk (*) indicates significant different from control ($p<0.05$).

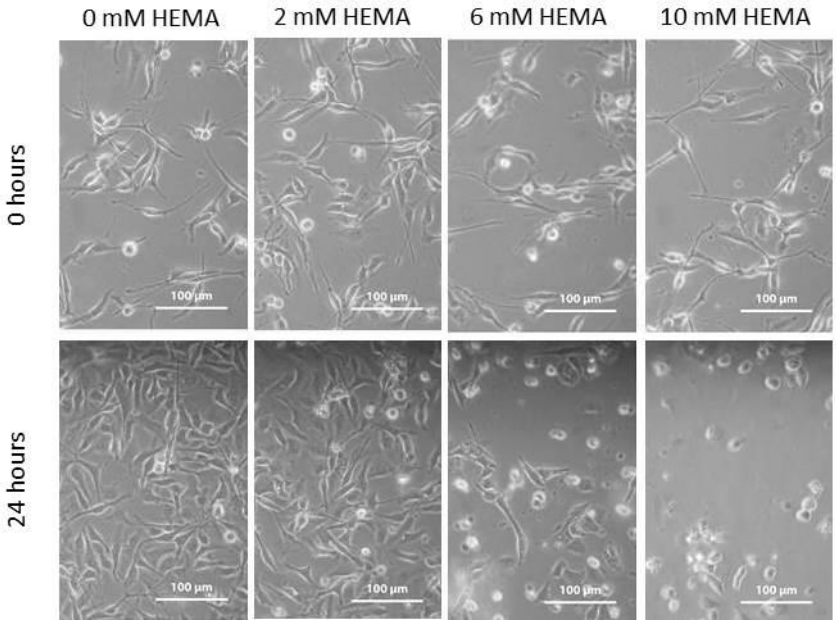

Figure 4-2: Phase-contrast microscopy images taken of BEAS-2B cells after 0 and 24 hours exposure to HEMA.

4.1.2 Effects of BSO on cell viability

Cells exposed to 5-100 µM BSO showed no significant change when compared to control (Figure 4-3).

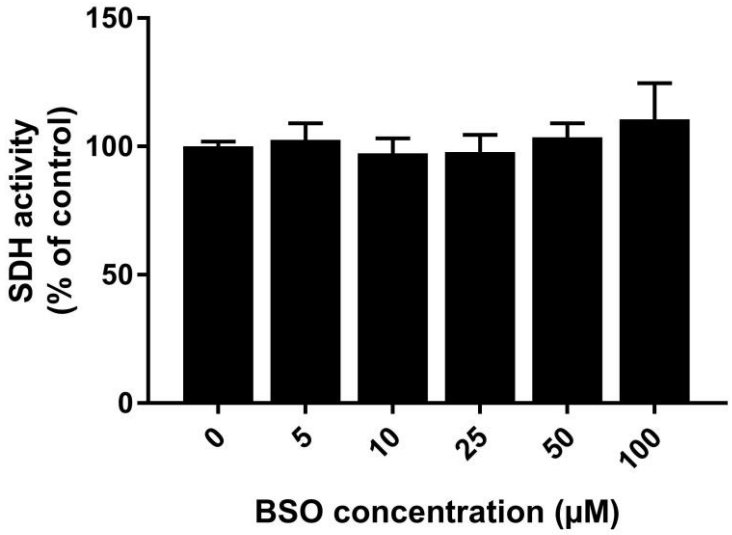

Figure 4-3: Cell viability determined as SDH activity in BEAS-2B cells after 24 hours exposure to BSO. Results are ahown as percentage of control (mean ± SD, n=4).

4.2 Cell Death

Cell death was determined by fluorescence microscopy. BEAS-2B cells were stained with PI and Höecst 33342 after 24 hours of exposure to different concentrations of HEMA. 300 cells were counted and categorized as viable, necrotic or apoptotic.

4.2.1 Effects of HEMA on cell death

The portion of apoptotic (figure 4-4) and necrotic (figure 4-5) cells seemed to increase with increasing HEMA concentration, although not significantly.

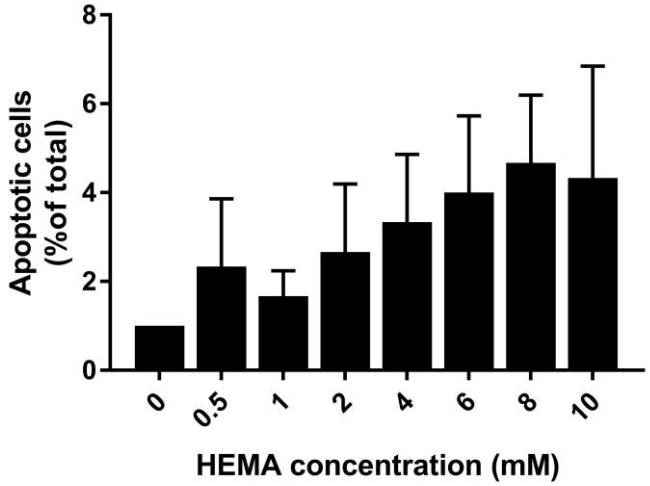

Figure 4-4: Cell death measurement by fluorescence microscopy of BEAS-2B cells after 24 hours exposure to HEMA. Results are shown as percentage of total (mean ± SD, n=3).

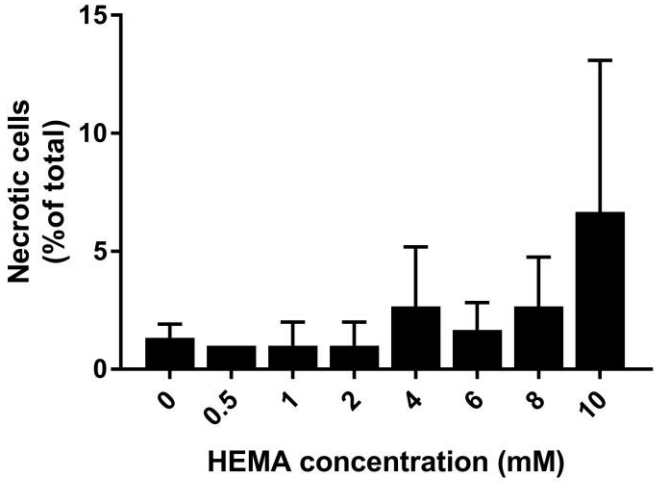

Figure 4-5: Cell death measurement by fluorescence microscopy of BEAS-2B cells after 24 hours exposure to HEMA. Results are shown as percentage of total (mean ± SD, n=3).

4.3 Cell growth

Cell cycle distribution was analysed using flow cytometry. BEAS-2B cells were exposed to different concentrations of HEMA and BSO for 24 hours before DNA-content was measured to determine the distribution of cells in G1-, S- and G2-phase. Control contained non-exposed cells.

4.3.1 Effects of HEMA on cell growth

HEMA exposure appeared to mainly affect the portion of cells in the G1- and S-phase (Figure 4-6). Cells exposed to 4 and 6 mM HEMA showed significant increase in portion of cells in S-phase when compared to control (Figure 4-7).

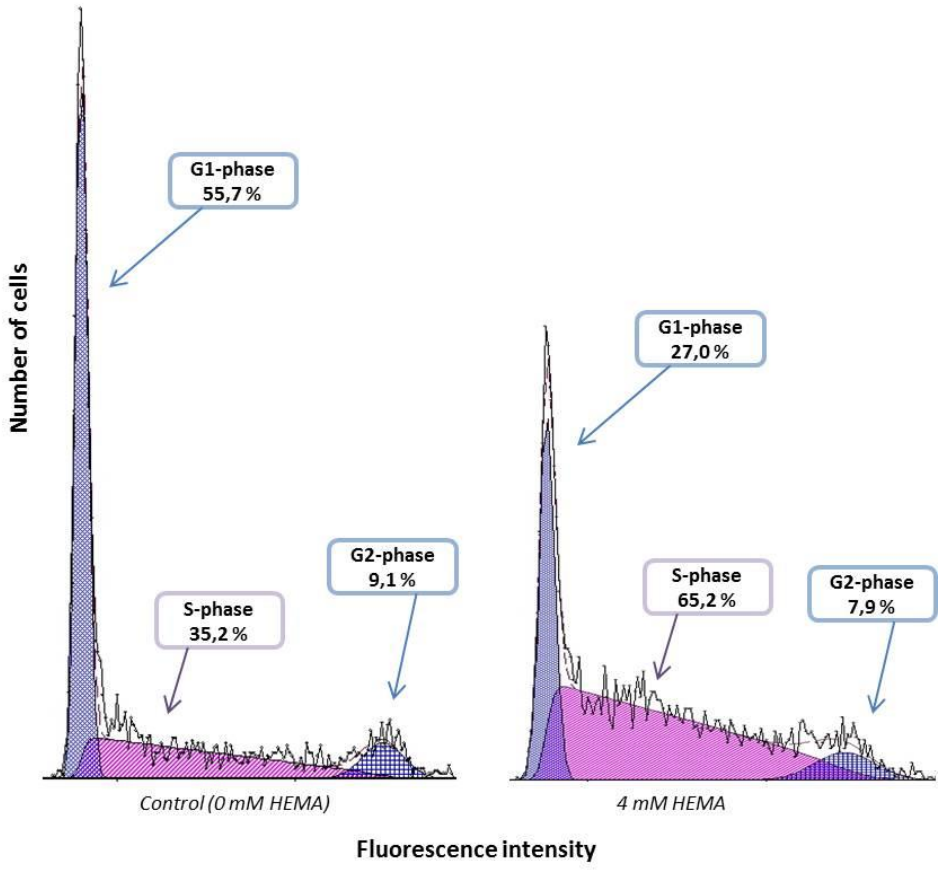

Figure 4-6: Representative histograms of cell cycle distribution of BEAS-2B cells exposed to 0 mM HEMA (control) and 4 mM HEMA.

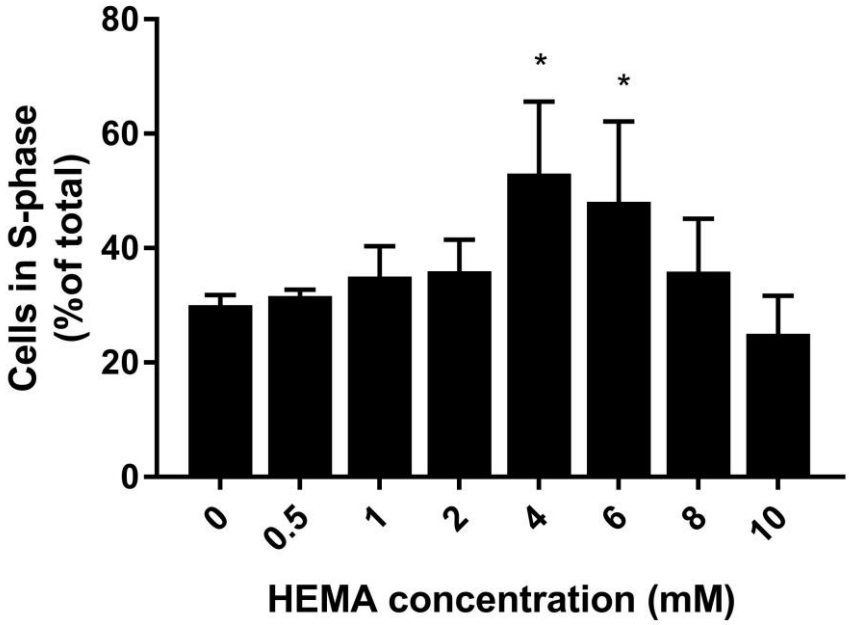

Figure 4-7: BEAS-2B cells in S-phase, categorized by measuring DNA-content with flow cytometry, after 24 hours exposure to HEMA. Results are shown as percentage of total (mean ± SD, n=3). Asterisk (*) indicates significant different from control ($p<0.05$).

4.3.2 Effects of BSO on cell growth

BSO exposure appered not to affect the portion of cells in the different phases (figure 4-8, figure 4-9).

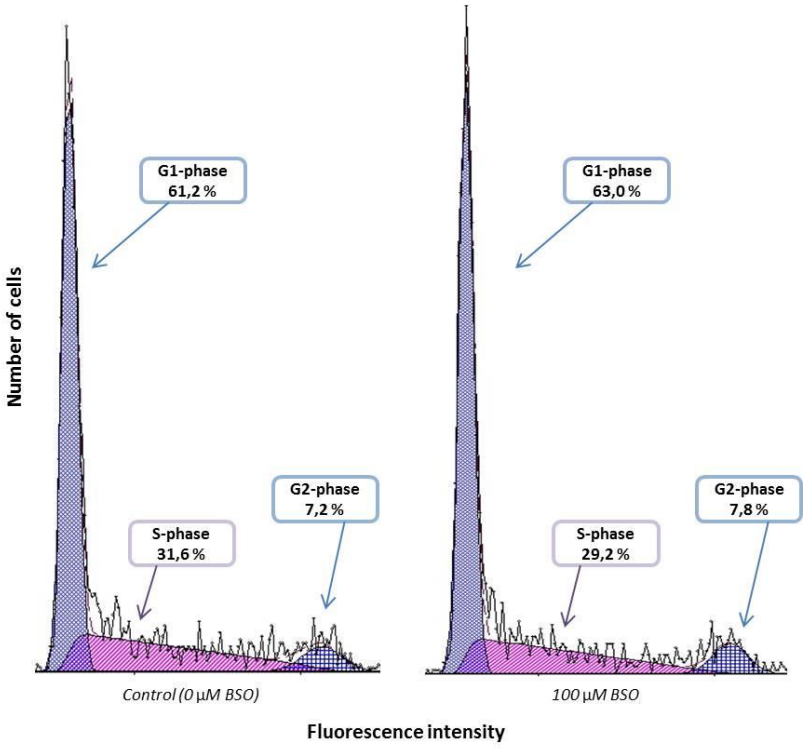

Figure 4-8: Representative histograms of cell cycle distribution of BEAS-2B cells exposed to 0 µM BSO (control) and 100 µM BSO.

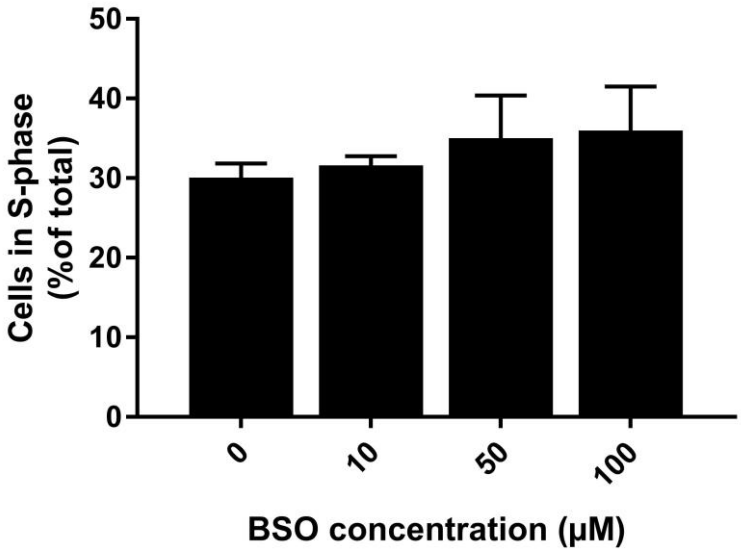

Figure 4-9: BEAS-2B cells in S-phase, categorized by measuring DNA-content with flow cytometry, after 24 hours exposure to HEMA. Results are shown as percentage of total (mean ± SD, n=3).

4.4 GSH-measurements

GSH-measurements were analysed using flow cytometry. BEAS-2B cells were exposed to different concentrations of HEMA or BSO for 4 and 8 hours before the cells were stained with mBrB. Control contained non-exposed cells.

4.4.1 Effects of HEMA on GSH-level

Cells exposed to 1-6 mM HEMA for 4 hours showed significant reduction in GSH-level compared to control (Figure 4-10). GSH-level in cells exposed to the same concentrations of HEMA for 8 hours showed a similar reduction (data not shown).

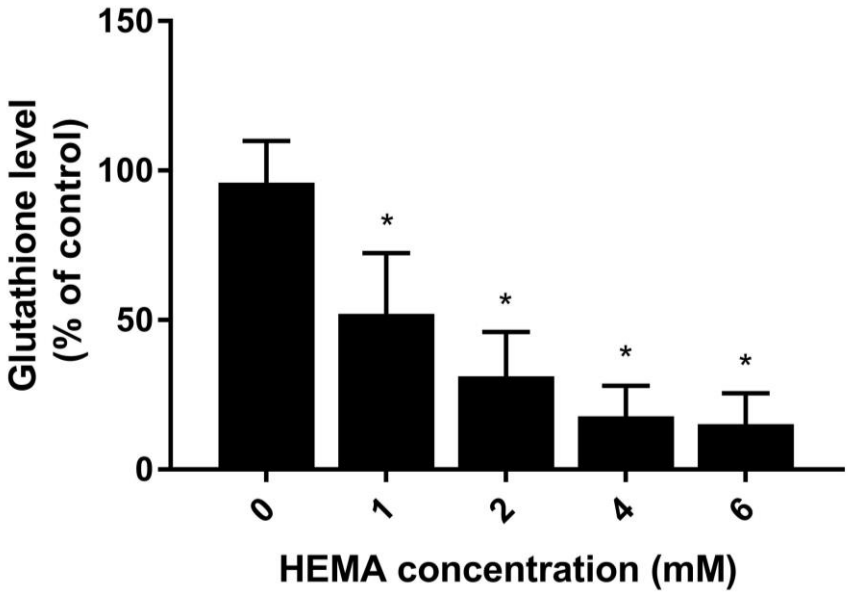

Figure 4-10: GSH-measurement by flow cytometry in BEAS-2B cells after 4 hours exposure to HEMA. Results are shown as percentage of control (mean ± SD, n=3). Asterisk (*) indicates significant different from control ($p<0.05$).

4.4.2 Effects of BSO on GSH-level

Cells exposed to 10, 50 and 100 µM BSO for 8 hours showed significant reduction in GSH-level compared to control (Figure 4-11). GSH-level in cells exposed to the same concentrations of BSO for 4 hours showed no reduction (data not shown).

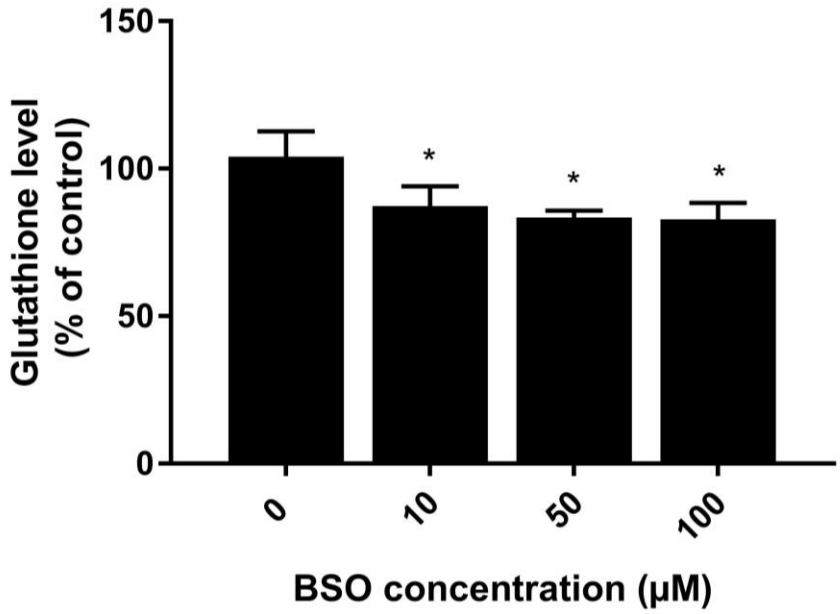

Figure 4-11: GSH-measurement by flow cytometry of BEAS-2B cells after 8 hours exposure to BSO. Results are shown as percentage of control (mean ± SD, n=3). Asterisk (*) indicates significant different form control ($p<0.05$).

4.5 Western blot

Western blot was used to determine the level of β-actin and S-glutathionylated proteins in BEAS-2B. Cells were exposed to 0 and 2 mM HEMA for 4, 6 and 8 hours and 0, 10, 50 and 100µM BSO for 6 and 8 hours. Nitrocellulose membranes were stained with Ponceau for visually inspection of the transfer of proteins before incubation of antibodies (figure 4-12). The membrane incubated with specific antibodies towards S-glutathionylated proteins showed a strong band with molecular weight between 37 and 50 kDa (figure 4-13 A). This band was used for further analysis. Membrane incubated with both specific antibodies towards S-glutathionylated proteins and β-actin (MW 42 kDa) detected protein with equal migration (figure 4-13 B). Controls contained non-exposed cells.

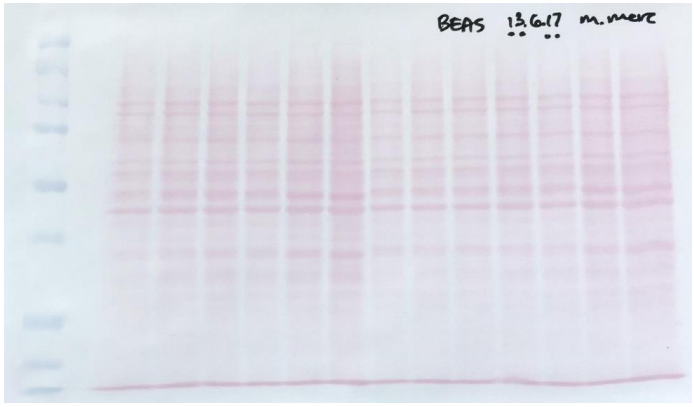

Figure 4-12: Ponceau-staining of nitrocellulose membrane. Molecule marker can be seen as blue lines (left).

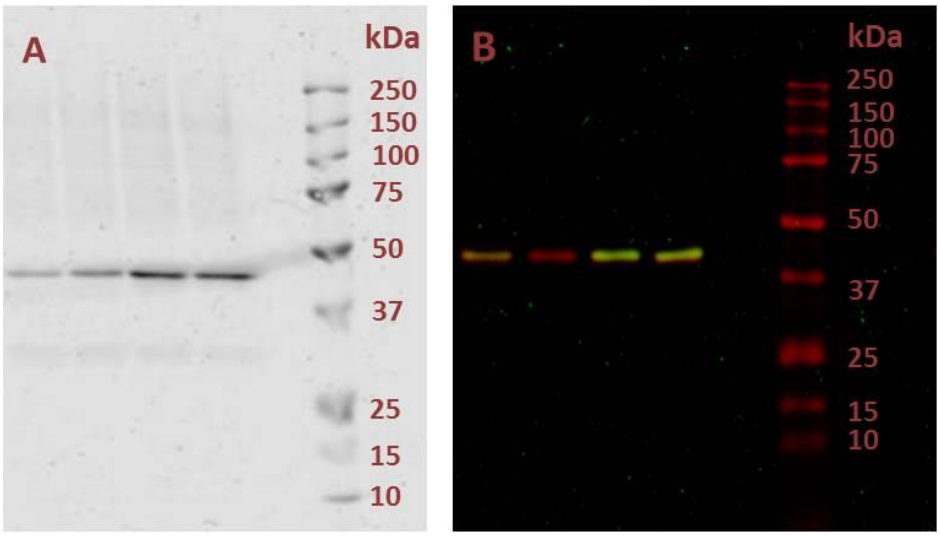

Figure 4-13: (A) Blot incubated with antibodies towards S-glutathionylated proteins. (B) Blot incubated with antibodies towards S-glutathionylated proteins (green) and β-actin (red). Molecule marker can be seen to the right in each picture with molecular sizes presented in kilo Dalton (kDa).

4.5.1 Effects of HEMA on S-glutathionylated proteins

Western blotting showed significant increased level of S-glutathionylated proteins with time in non-exposed control cells. This increase was not seen in cells exposed to 2 mM HEMA (figure 4-14).

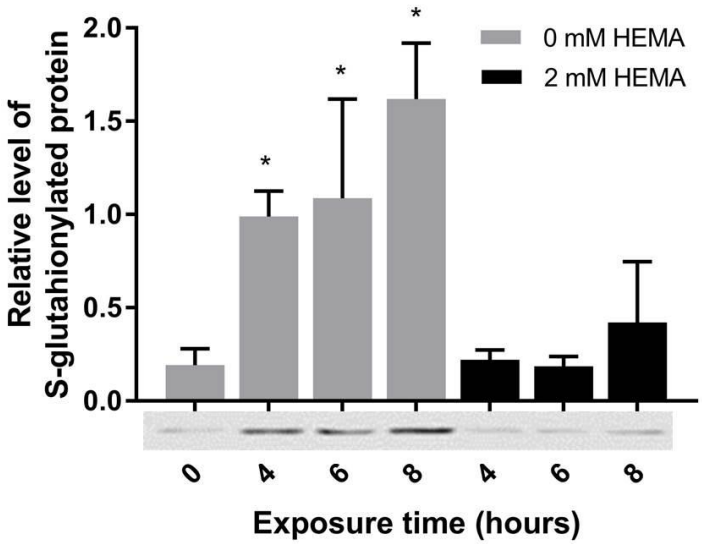

Figure 4-14: Levels of S-glutathionylated protein (MW approx. 42 kDa) in BEAS-2B cells (unexposed and exposed to 2 mM HEMA) measured by western blotting. Results are shown as relative levels to control 0 hours (mean ± SD, n=3). Asterisk (*) indicates significant different from control 0 hours ($p<0.05$). One representative blot is shown below bars.

4.5.3 Effects of BSO on S-glutathionylated proteins

Western blotting showed significant lower level of S-glutathionylated proteins in cells exposed to 10, 50 and 100µM BSO for 8 hours compared to control (figure 4-15). Cells exposed to the same concentrations of BSO for 6 hours showed no significant change compared to control (6 hours) (data not shown).

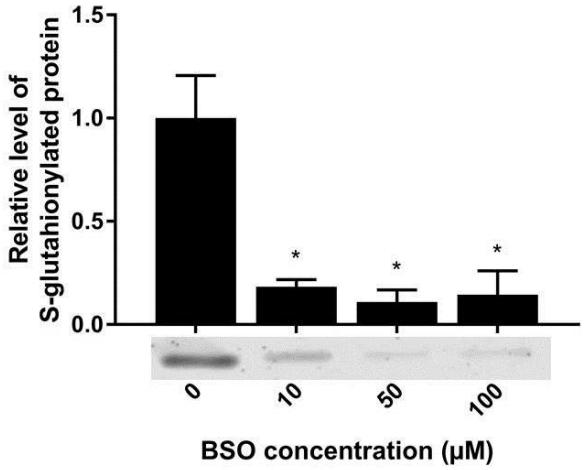

Figure 4-15: Levels of S-glutathionylated protein (MW approx. 42 kDa) in BEAS-2B cells (unexposed and exposed to 2 mM HEMA) measured by western blotting. Results are shown as relative levels to control (mean ± SD, n=3). Asterisk (*) indicates significant different from control ($p<0.05$). One representative blot is shown below bars.

4.5.2 Effects of HEMA on β-actin

Western blotting showed no significant difference in levels of β-actin in non-exposed cells and cells exposed to 2 mM HEMA compared to control (0 hours) (figure 4-16).

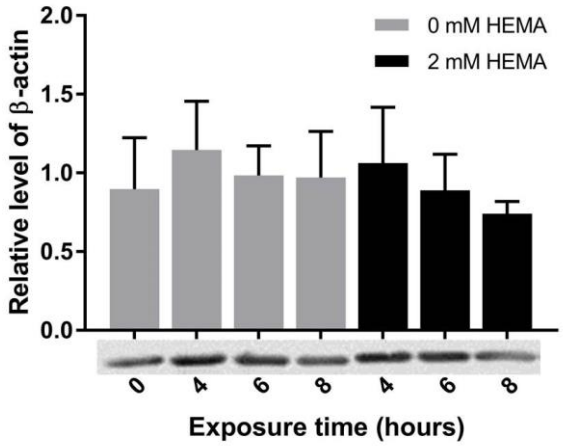

Figure 4-16: Levels of β-actin (MW 42 kDa) in BEAS-2B cells (unexposed and exposed to 2 mM HEMA) measured by western blotting. Results are shown as relative levels to control 0 hours (mean ± SD, n=3). One representative blot is shown below bars.

4.6 Immunofluorescence

Immunofluorescence was used to study β-actin, S-glutathionylated proteins and F-actin in BEAS-2B cells. Cells were exposed to 0 and 2 mM HEMA for 6 hours, before being fixed and stained with specific antibodies or phalloidin together with DAPI. Controls contained non-exposed cells.

4.6.1 Effects of HEMA on β-actin

Cells incubated with specific antibodies towards β-actin showed staining throughout the cytoplasma of the cell. No change between control and cells exposed to 2 mM HEMA were observed (figure 4-17).

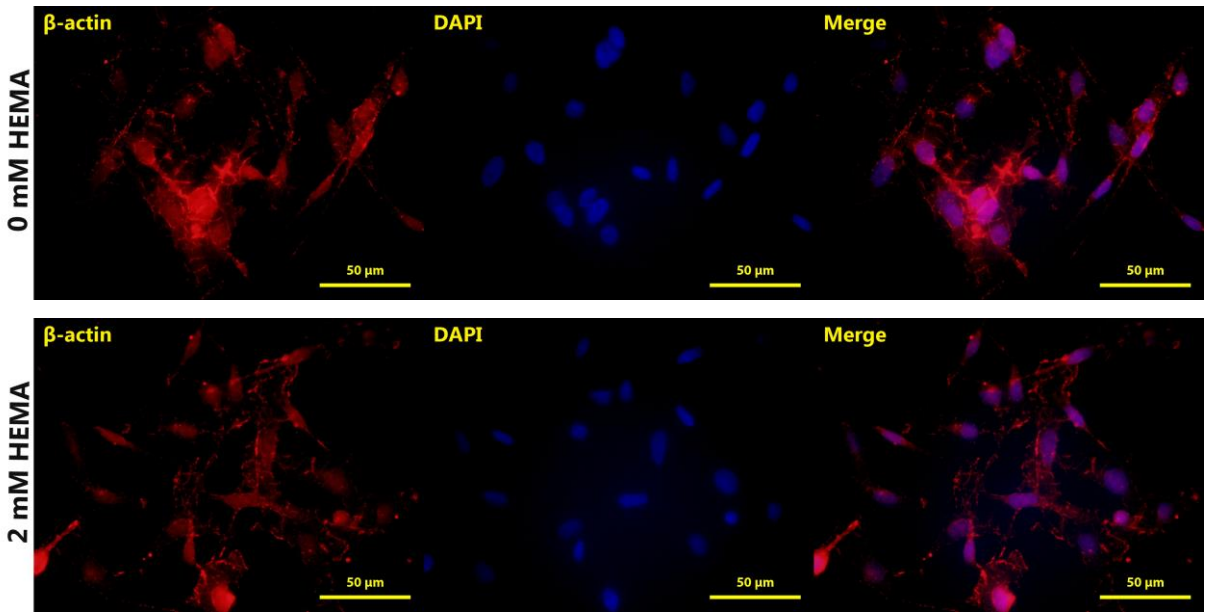

Figure 4-17: Immunofluorescence images of BEAS-2B cells after 6 hours exposure to HEMA. Cells were stained with specific antibodies towards β-actin (red) and nucleus is stained with DAPI (blue). Images merged to the right.

4.6.2 Effects of HEMA on S-glutathionylated proteins

Cells incubated with specific antibodies towards S-glutathionylated proteins showed staining throughout the cytoplasma of the cell. No change between control and cells exposed to 2 mM HEMA were observed (figure 4-18).

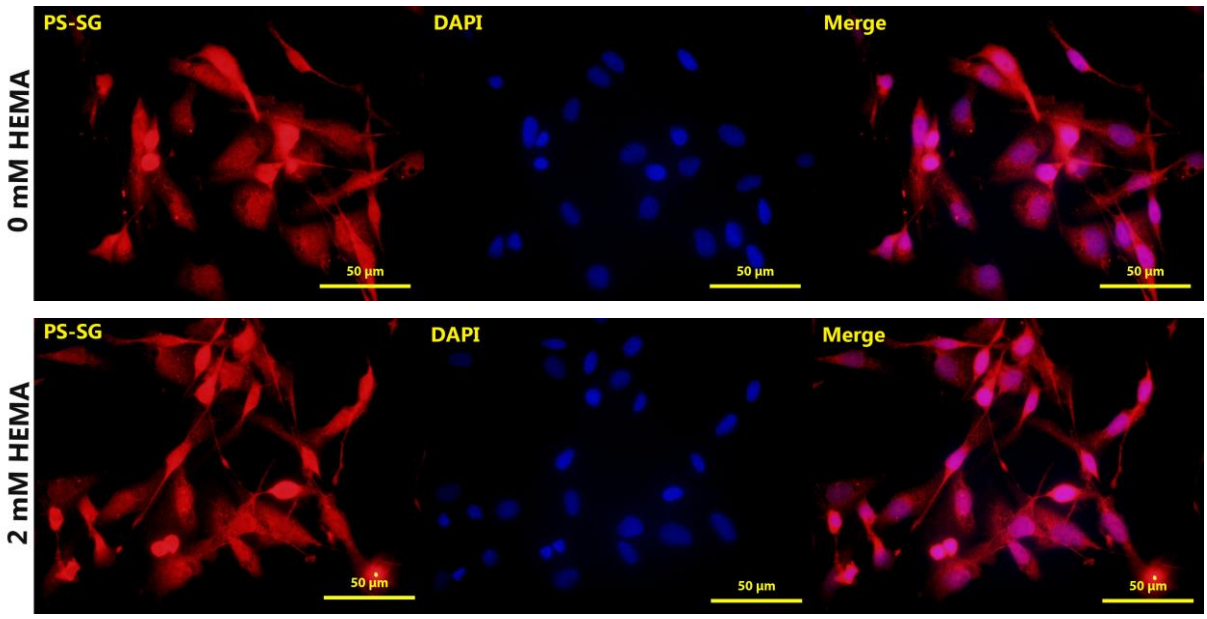

Figure 4-18: Immunofluorescence images of BEAS-2B cells after 6 hours exposure to HEMA. Cells were stained with specific antibodies towards S-glutathionylated proteins (PS-SG) (red) and nucleus is stained with DAPI (blue). Images merged to the right.

4.6.3 Effects of HEMA on F-actin

Cells incubated with phalloidin that specifically binds F-actin showed filament structures throughout the cytoplasma of the cell. No change between control and cells exposed to 2 mM HEMA were observed (figure 4-19).

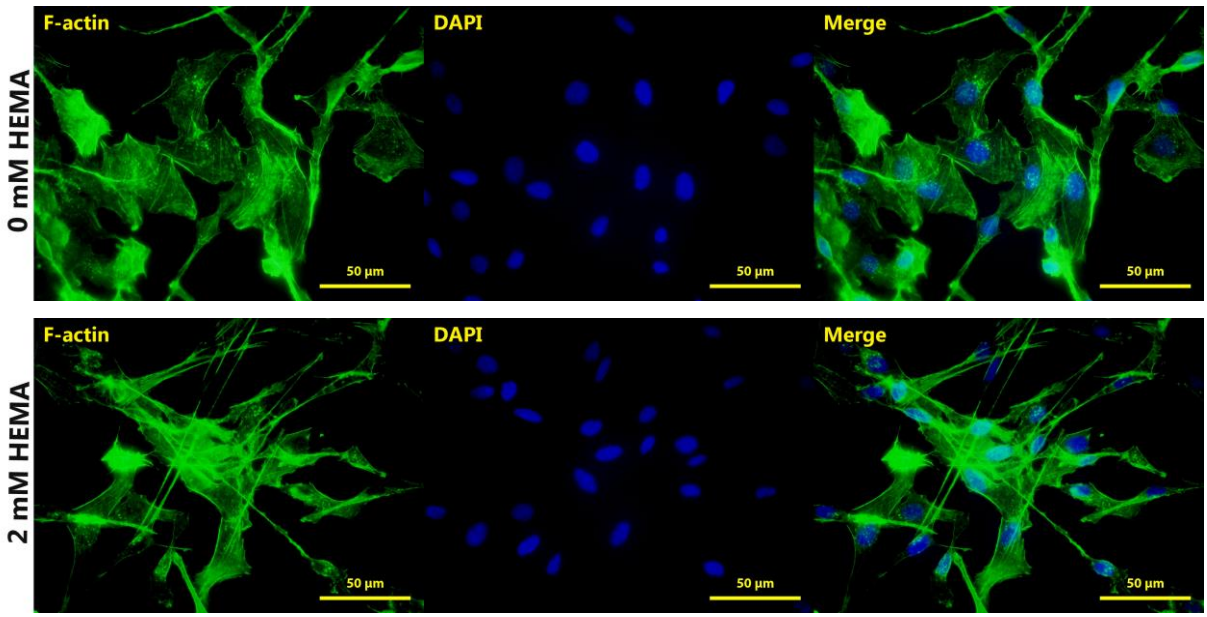

Figure 4-19: Immunofluorescence images of BEAS-2B cells after 6 hours exposure to HEMA. Cells were stained with phalloidin that specifically binds F-actin (green) and nucleus is stained with DAPI (blue). Images merged to the right.

4.7 Peptide analysis

LC-MS was used to investigate the ability of HEMA to spontaneously bind to different synthetic peptides based on the last 14 AA in the carboxyl-terminus of β-actin (table 3-2). Synthetic peptides were incubated with 0 and 2 mM HEMA for 24 hours before being analysed.

4.7.1 Synthetic peptide

Synthetic peptide incubated with 0 mM HEMA, showed one peak in the total ion chromatogram (TIC) eluting at 1.460 minutes. The mass of the observed ions corresponded with the theoretical mass of the peptide as reported by GenScript (table 4-1, figure 4-20). Upon incubation with 2 mM HEMA, an additional peak eluting at 1.549 minutes was observed in the TIC. The MS fragmentation pattern suggested the formation of a peptide + HEMA adduct (table 4-1, figure 4.21).

Tabell 4-1: List of ionic species (m/z) observed for synthetic peptide incubated with 0 and 2 mM HEMA. Theoretical MW (g/mol) is from GenScript. Retention time (rt) for peaks with observed mass fragmentation ions (m/z) and suggested identification.

Sample	Theoretical MW (g/mol)	Incubation	pH	Peak	rt (min)	Observed MS fragmentation (m/z)	Identification
Synthetic peptide	1637.7	0 mM HEMA	7.9	1	1.460	410.3 [M+4H]4+ 546.8 [M+3H]3+	Synthetic peptide
Synthetic peptide	1637.7	2 mM HEMA	7.9	1	1.460	410.3 [M+4H]4+ 546.9 [M+3H]3+	Synthetic peptide
				2	1.549	443.0 [M+4H]4+ 590.2 [M+3H]3+	Synthetic peptide + HEMA

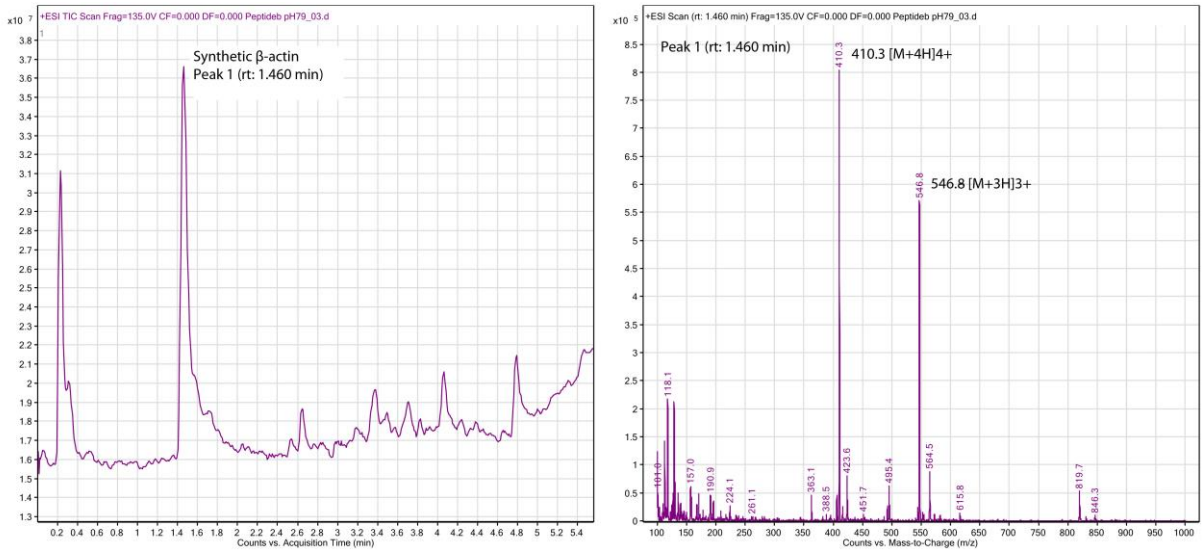

Figure 4-20: Total ion chromatogram (TIC) of synthetic peptide incubated with 0 mM HEMA and MS-spectrum of peak 1 (rt: 1.460 min).

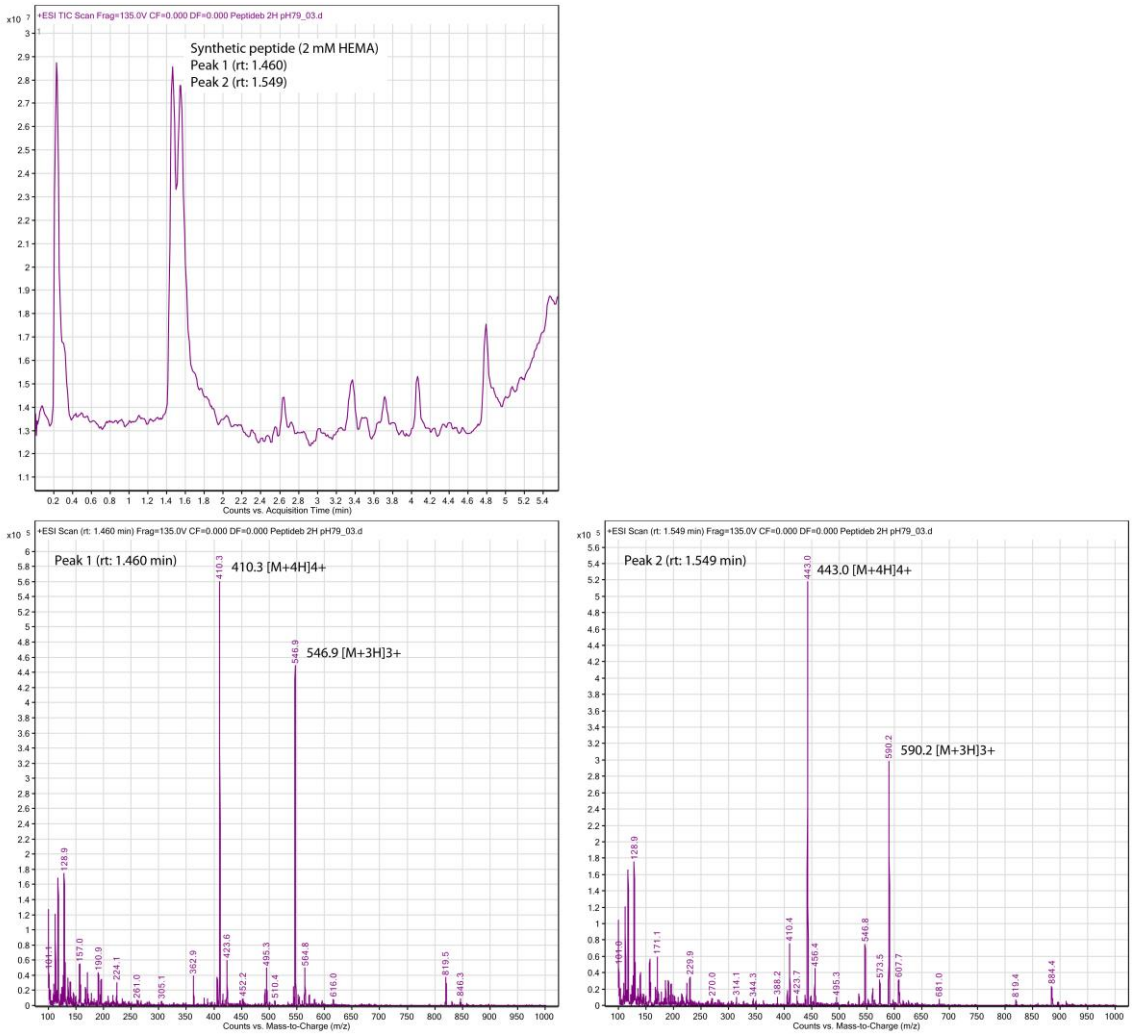

Figure 4-21: Total ion chromatogram (TIC) of synthetic peptide incubated with 2 mM HEMA and MS-spectra of peak 1 (rt: 1.460 min) and peak 2 (rt: 1.549 min).

4.7.2 Synthetic peptide without cysteine

Synthetic peptide without cysteine incubated with 0 and 2 mM HEMA, both showed one peak in the total ion chromatogram (TIC) eluting at 1.351 and 1.361 minutes, respectively. The mass of the observed ions corresponded with the theoretical mass of the peptide as reported by GenScript (table 4-2, figure 4-22, figure 4-23).

Table 4-2: List of ionic species (m/z) observed for synthetic peptide without cysteine (C) incubated with 0 and 2 mM HEMA. Theoretical MW (g/mol) is from GenScript. Retention time (rt) for peaks with observed mass fragmentation ions (m/z) and suggested identification.

Sample	Theoretical MW (g/mol)	Incubation	pH	Peak	rt (min)	Observed MS fragmentation (m/z)	Identification
Synthetic peptide without C	1534.8	0 mM HEMA	7.9	1	1.361	384.6 [M+4H]4+ 512.5 [M+3H]3+	Synthetic peptide without C
Synthetic peptide without C	1534.8	2 mM HEMA	7.9	1	1.351	384.6 [M+4H]4+ 512.5 [M+3H]3+	Synthetic peptide without C

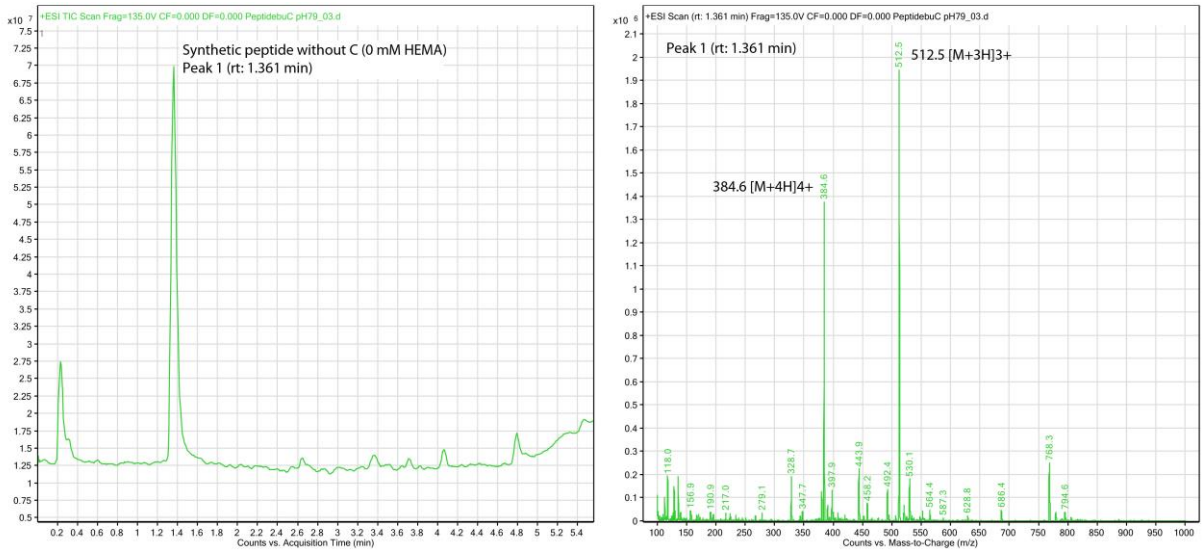

Figure 4-22: Total ion chromatogram (TIC) of synthetic peptide wihtout cycteine (C) incubated with 0 mM HEMA and MS-spectrum of peak 1 (rt: 1.361 min).

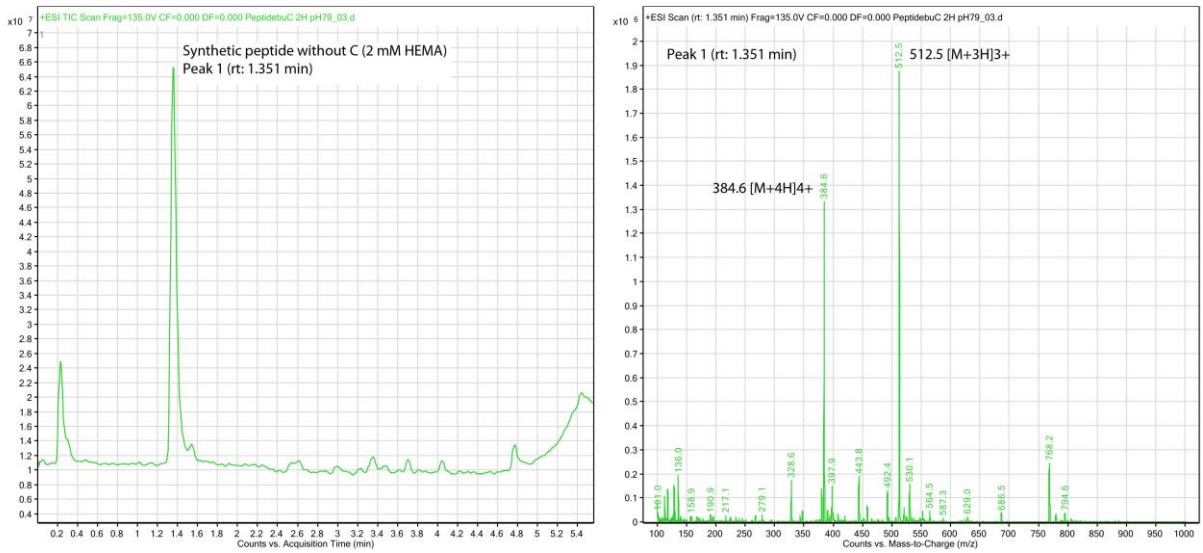

Figure 4-23: Total ion chromatogram (TIC) of synthetic peptide wihtout cycteine (C) incubated with 2 mM HEMA and MS-spectrum of peak 1 (rt: 1.351 min).

4.7.3 Synthetic peptide without lysine

Synthetic peptide without lysine incubated with 0 mM HEMA, showed one peak in the total ion chromatogram (TIC) eluting at 1.647 minutes. The mass of the observed ions corresponded with the theoretical mass of the peptide as reported by GenScript (table 4-3, figure 4-24). Upon incubation with 2 mM HEMA, an additional peak eluting at 1.716 minutes was observed in the TIC. The MS fragmentation pattern suggested the formation of a peptide + HEMA adduct (table 4-3, figure 4-25).

Table 4-3: List of ionic species (m/z) observed for synthetic peptide without lysine (K) incubated with 0 and 2 mM HEMA. Theoretical MW (g/mol) is from GenScript. Retention time (rt) for peaks with observed mass fragmentation ions (m/z) and suggested identification.

Sample	Theoretical MW (g/mol)	Incubation	pH	Peak	rt (min)	Observed MS fragmentation (m/z)	Identification
Synthetic peptide without K	1509.5	0 mM HEMA	7.9	1	1.647	504.2 [M+3H]3+	Synthetic peptide without K
Synthetic peptide without K	1509.5	2 mM HEMA	7.9	1	1.647	504.1 [M+3H]3+	Synthetic peptide without K
				2	1.716	547.5 [M+3H]3+	Synthetic peptide without K + 1 HEMA

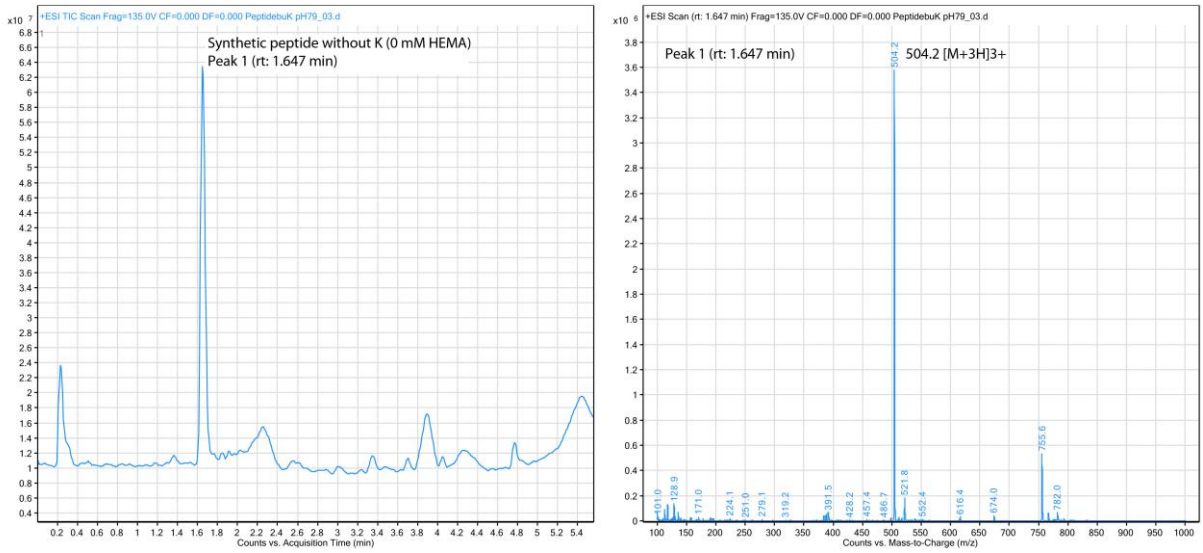

Figure 4-24: Total ion chromatogram (TIC) of synthetic peptide without lysine (K) incubated with 0 mM HEMA and MS-spectrum of peak 1 (rt: 1.647 min).

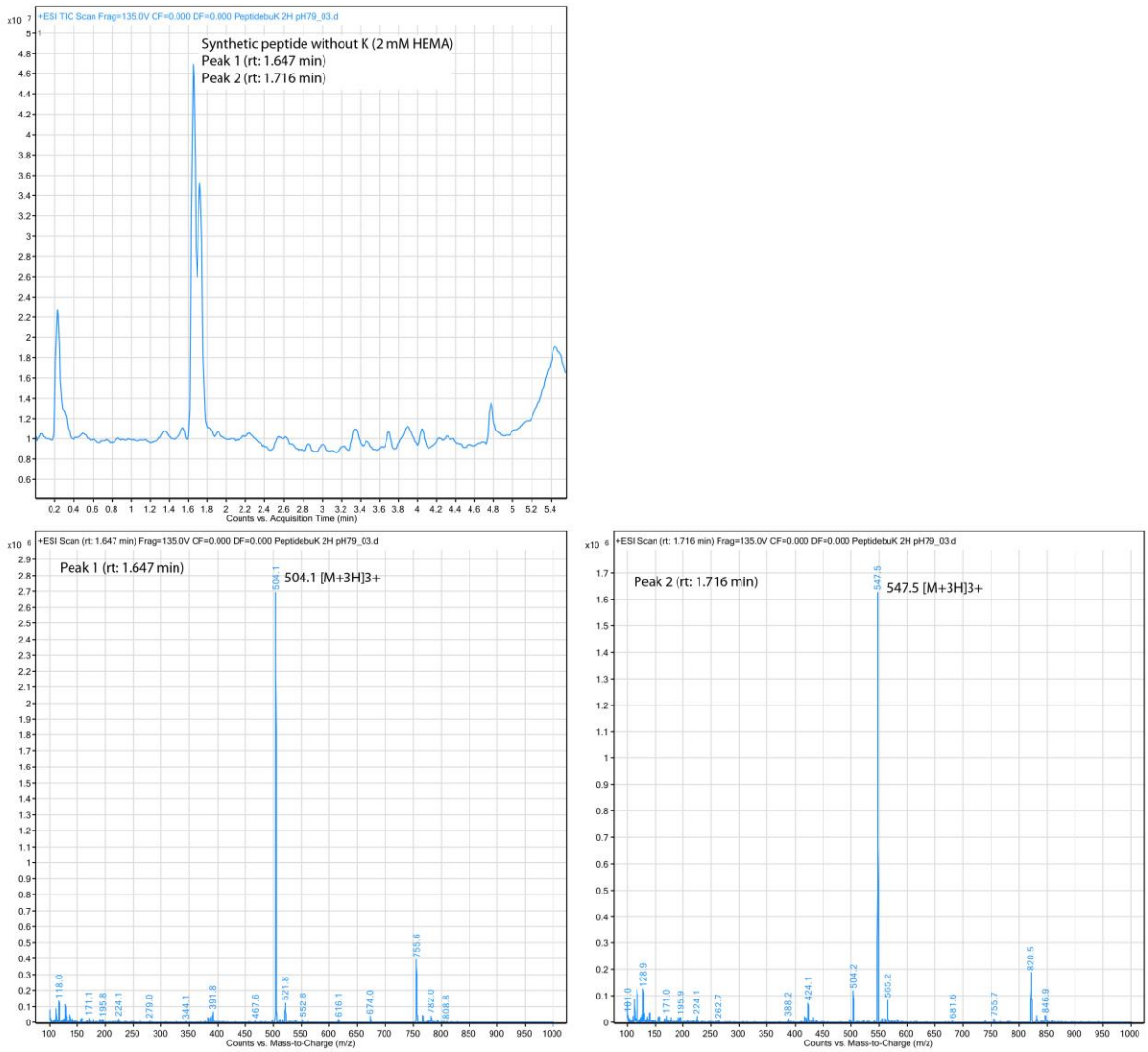

Figure 4-25: Total ion chromatogram (TIC) of synthetic peptide without lysine (K) incubated with 2 mM HEMA and MS-spectra of peak 1 (rt: 1.647 min) and peak 2 (rt: 1.716 min).

4.7.4 Synthetic peptide without cysteine and lysine

Synthetic peptide without cysteine and lysine incubated with 0 and 2 mM HEMA, both showed one peak in the total ion chromatogram (TIC) eluting at 1.549 minutes. The mass of the observed ions corresponded with the theoretical mass of the peptide as reported by GenScript (table 4-4, figure 4-26, figure 4-27).

Table 4-4: List of ionic species (m/z) observed for synthetic peptide without cysteine (C) and lysine (K) incubated with 0 and 2 mM HEMA. Theoretical MW (g/mol) is from GenScript. Retention time (rt) for peaks with observed mass fragmentation ions (m/z) and suggested identification.

Sample	Theoretical MW (g/mol)	Incubation	pH	Peak	rt (min)	Observed MS fragmentation (m/z)	Identification
Synthetic peptide without C and K	1406.1	0 mM HEMA	7.7	1	1.549	469.7 [M+3H]3+	Synthetic peptide without C and K
Synthetic peptide without C and K	1406.1	2 mM HEMA	7.7	1	1.549	469.7 [M+3H]3+	Synthetic peptide without C and K

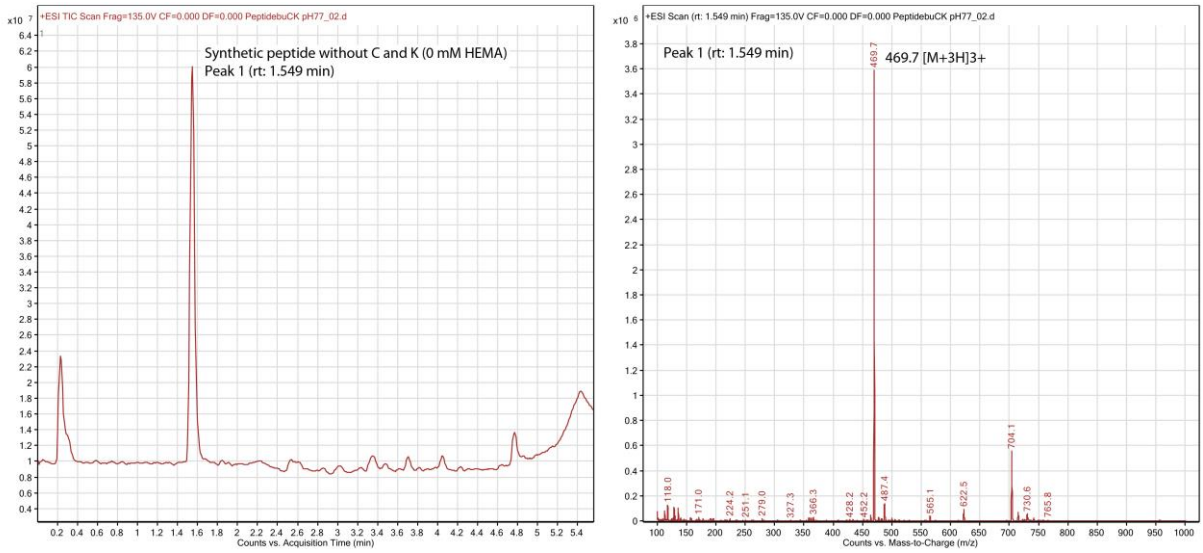

Figure 4-26: Total ion chromatogram (TIC) of synthetic peptide without cysteine (C) and lysine (K) incubated with 0 mM HEMA and MS-spectrum of peak 1 (rt: 1.549 min).

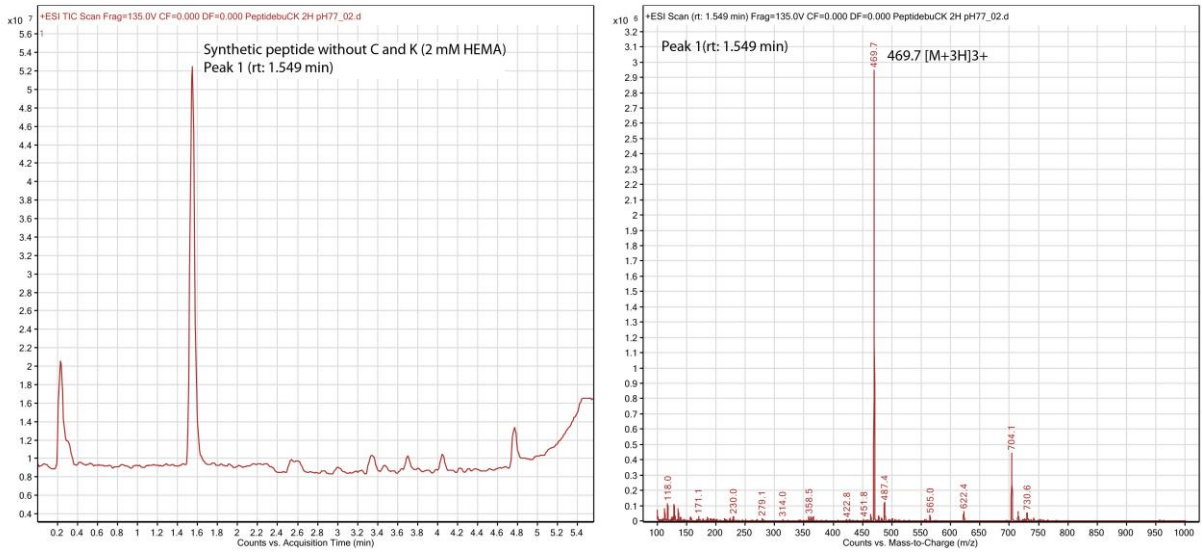

Figure 4-27: Total ion chromatogram (TIC) of synthetic peptide without cysteine (C) and lysine (K) incubated with 2 mM HEMA and MS-spectrum of peak 1 (rt: 1.549 min).

5 Discussion

Both dental personnel and patients are exposed to methacrylate monomers present in resin-based dental materials (26, 27, 79). Methacrylates are shown to have a toxic potential *in vitro*, but knowledge regarding the detailed molecular interactions that lead to the observed toxic response is scarce. Hence, consequences of exposure in a clinical situation are difficult to predict. One of the most studied methacrylate monomers *in vitro* is HEMA. Although the cause of observed cytotoxic response *in vitro* is not clear, GSH depletion and elevated ROS-levels are suggested to be of importance (33, 34). In this study, an *in vitro* cell line model (BEAS-2B) was chosen to investigate possible interaction between HEMA and other cellular components. Results showed that HEMA is cytotoxic to BEAS-2B cells at 4 mM and above. Further, HEMA was shown to decrease cellular GSH-levels and affects protein S-glutathionylation of at least one protein (MW approximately 42 kDa). These observations were also evident at concentrations below 4 mM. Finally, LC-MS studies using synthetic peptides indicated a direct interaction of HEMA with cysteine (374) in β-actin.

5.1 Methodological considerations

5.1.1 Choice of model system

For this study, a homogenous immortalised cell line was used as a model system. A bronchial epithelial cell line was chosen due to the knowledge of airways as an important route for methacrylate exposure (26, 27). Although such models cannot imitate the complexity of living organisms, *in vitro* studies are usually preferred when considering aspects of ethics, cost, accessibility and easy-to-implement methodology. These studies provide useful information of processes affected in living cells, but care must be taken when translating the results to an *in vivo* situation.

The concentrations of HEMA used in this study were higher than concentrations measured in saliva retrieved from patients treated with HEMA-containing materials (20). Concentrations of HEMA measured in air, close to dental personnel and patients are also low compared to the concentrations used in this study (26). However, concentration in the lung surfactant that airway cells are exposed to do not merely depend on air concentrations. No data concerning how easily methacrylates are

dissolved in lung surfactant has been reported. *In vitro* studies have shown that HEMA has the ability to diffuse through dentin (80) and that methacrylates in cured materials are known to leak out over time (20, 21). This gives the possibility of a cumulative exposure over time that is suggested to be of importance regarding effects of methacrylate monomers (81). The limited ability to measure the effect of long-time exposure in cell-line models encourages the use of other approaches. Knowledge of initial molecular interactions can provide indications of long-term effects. In line with this strategy, monitoring of spontaneous reactions between HEMA and cellular components was the focus of this thesis.

Because actin dynamics is reported to depend on S-glutathionylation (61, 64, 69), HEMA exposure conditions that lead to changes in the cytoskeleton may indirectly affect actin S-glutathionylation. The cytoskeleton is a structure that will change during cellular processes, such as cell cycle progression or apoptosis (62, 63). One main goal of this study was to investigate if HEMA affects thiol-dependent cellular processes directly. Hence, exposure conditions that alters cell growth and induces cell death should be avoided. In cells exposed to 2 mM HEMA and below we could not detect any changes in these processes. Thus, the effect seen on GSH-depletion and changes in protein S-glutathionylation is not likely to be a consequence of such changes in the cytoskeleton.

5.1.2 Choice of methods

Most methods used to detect cytotoxicity have their limitations, but in combination they can achieve a comprehensive overview. In this study, the toxicity of HEMA on BEAS-2B cells was measured with the combination of the MTT-assay, visual investigation with phase-contrast microscopy, cell death counting (necrotic and apoptotic cells) with fluorescence microscopy and cell cycle analysis with flow cytometry. MTT-assay is a fast and easy screening method to observe the density of viable cells. Changes may both depend on alterations in cell death and cell growth. Therefore, cell death counting and cell cycle analysis were performed to support the results from the MTT-assay.

BSO alters the GSH concentration by inhibiting an enzyme required for GSH-production (71). This gives a reduction of GSH-concentration by a different mechanism than what is

suggested for HEMA and gives an opportunity to investigate if GSH-depletion is involved with changes in protein S-glutathionylation. However, the time taken for the concentration of GSH to decrease may vary for these mechanisms and should be taken into consideration. In this study, BSO-exposure towards cells was incorporated in the MTT-assay, cell growth- and GSH-measurements, as well as western blotting when looking at S-glutathionylated proteins.

Western blot incubated with a specific antibody towards S-glutathionylated proteins showed one strong band with molecular weight of approximately 42 kDa. Membranes stained with specific antibodies towards β-actin and S-glutathionylated proteins detected proteins with equal migration. With the knowledge that β-actin is a highly S-glutathionylated protein(60), the observed band on western blot is likely β-actin. To further investigate the effect of HEMA on the S-glutathionylation site (cys374) in β-actin, peptides based on the last 14 AA of the carboxyl-terminus of β-actin and containing cys374 were purchased. In addition, this AA-sequence also contains lysine, and HEMA has been hypothesised to form adducts with both cysteine and lysine residues in proteins spontaneously (35, 36, 82). Based on these assumptions, four synthetic peptides with different AA-sequences were designed; one with all 14 amino acids, one without cysteine, one without lysine and one without both cysteine and lysine. The peptides were incubated with HEMA and analysed using LC-MS.

5.2 Discussion of results

As an initial assessment, the cytotoxic effect of HEMA on BEAS-2B cells was investigated. HEMA showed a reduction of cell viability, as measured by MTT. Supporting the reduction in MTT-conversion, visual investigation of BEAS-2B cells indicated fewer cells in a dose-dependent manner. Measurement of DNA in BEAS-2B cells showed an increase of cells in the S-phase. In combination with the result indicating fewer cells, the increase in S-phase is due to slower progression through this phase. Delay or arrest during cell cycle progression is usually due to an error detected in the cell (49). This indicates that HEMA induces damage in the cell, which inhibits the cell to progress further through the cell cycle. Increasing HEMA concentrations also seemed to increase the portion of apoptotic and necrotic cells, although this increase was not significant. The results indicating both increased cell death and cell growth disruption, correlate well with

previously reported studies (29, 32). No changes in viability, cell death or cell growth pattern was observed in cells exposed to 2 mM HEMA and below. Using the same combination of methods, no changes were seen at any of the investigated BSO-concentrations.

GSH depletion was measured with flow cytometry of mBrB-stained cells. HEMA-exposure (1-6 mM) resulted in a significant and concentration-dependent GSH-depletion, as seen in other studies (16, 33). Cells exposed to BSO (10-100 μM) for 8 hours also induced a significant depletion of GSH. The pattern of S-glutathionylation of one protein with a molecular weight of approximately 42 kDa was different in HEMA-exposed cells compared to control cells. The observed increase in protein S-glutathionylation in control cells indicate that S-glutathionylation is a sensitive modification of proteins that is affected by small changes in the cell culture conditions. This is beyond the scope of this study, but should be investigated further. In HEMA-exposed cells, however, the level of S-glutathionylated proteins remained unchanged. In cells exposed to BSO for 8 hours, the levels of protein S-glutathionylation were altered in the same way as in HEMA-exposed cells. These observations indicate that GSH-depletion, at least partly, is responsible for the effect of HEMA on protein S-glutathionylation.

S-Glutathionylation of β-actin is reported to inhibit the polymerisation of F-actin (64, 67) and thereby alter the actin dynamics and mechanics, which is essential for the cells mobility and organization (66, 68). This gave reason to expect a visual difference in F-actin between HEMA-exposed and non-exposed cells. The staining of cells with phalloidin that specifically stains F-actin and specific antibodies towards β-actin and S-glutathionylated proteins could not prove any effect of HEMA. However, immunofluorescence is not well suited as a quantitative method and care should be taken when interpreting the results. Another factor that may be of importance, is the time required for a potential effect on the cytoskeleton to occur in HEMA-exposed cells. In this study, the immunostaining was only carried out after 6 hours.

Results from the LC-MS studies showed that the molecular weight of peptides with cysteine in the AA-sequence increased by the mass of HEMA (130 g/mol). For peptides without cysteine incubated with HEMA, no increase in mass was observed. An adduct

formation between cys374 in β-actin and HEMA is likely to affect the S-glutathionylation. This type of competitive binding may provide an additional explanation for decreased protein S-glutathionylation in HEMA-exposed cells. The synthetic peptides also contained lysine, another well-known nucleophilic amino acid. The reported binding of HEMA to lysine (36) could not be confirmed in this study. It is important to emphasize that these measurements are done in a cell-free system with synthetic peptide representing only a small part of the protein. The peptides lack the influence of the remaining AA-sequence of the protein that may affect the availability of cys374 in living cells. Removal of an AA from the sequence will change the environment of the neighbouring AA and this may influence a potential adduct formation. Hence, the adduct formation with lysine cannot be ruled out in the case of lys373.

This is an *in vitro* study and care should be taken when translating the effects to *in vivo*. However, effects found on the molecular level *in vitro* are more likely transferable compared to more complex observations such as cell growth and regulated cell death. Assuming that the dynamics of actin is altered by HEMA-exposure, one could speculate that this effect may influence important processes like phagocytosis and wound-healing.

6 Conclusion

Within the limits of this study it can be concluded that:

- HEMA lowers the level of S-glutathionylation in BEAS-2B cells
- It is likely that the main protein affected is β-actin
- Both altered GSH-level and competitive binding of HEMA to the S-glutathionylation site of β-actin may explain this effect

7 Future perspectives

The results of this study indicate interesting effects of HEMA that could be of clinical relevance. To further verify these findings, additional studies should be carried out. In this study, the spontaneous adduct formation between cysteine and HEMA was observed using synthetic peptides in a cell-free system. To investigate if a parallel reaction between HEMA and cys374 in β-actin occurs in living cells, proteins should be extracted from HEMA-exposed cells and analysed. This work has been started, but due to time restrictions it was not possible to finish and include it in this study. If an effect of HEMA on the cytoskeleton is delayed compared to protein S-glutathionylation, a visual effect may need more than 6 hours to develop. Therefore, additional time-points should be investigated. Alternatively, stimulating cell migration by the use of a scratch-assay could detect changes in actin dynamics. Preliminary studies have indicated reduced migration of cells exposed to HEMA.

8 References

1. Hildebrand HF. Biomaterials – a history of 7000 years. BioNanoMaterials. 2013;14(3):119-33.
2. Park J, Lakes RS, SpringerLink. Biomaterials : An Introduction: Springer New York; 2007. p. 2-7
3. Sunnegårdh-Grönberg K, van Dijken JWV, Funegård U, Lindberg A, Nilsson M. Selection of dental materials and longevity of replaced restorations in Public Dental Health clinics in northern Sweden. Journal of Dentistry. 2009;37(9):673-678.
4. Kopperud HBM, Finger WJ, Hørsted-Bindslev P. Moderne tannfargede fyllingsmaterialer. Den norske tannlegeforenings tidende. 2011;121:34-39.
5. Miljøverndepartementet. Forbyr kvikksølv i produkter. In: Regjeringen Stoltenberg II: Miljøverndepartementet; 2007.
6. Reichl FX, Seiss M, Kleinsasser N, Kehe K, Kunzelmann KH, Thomas P, et al. Distribution and Excretion of BisGMA in Guinea Pigs. Journal of Dental Research. 2008. p. 378-380.
7. Arenholt-Bindslev D, Arenholt-Bindslev D, SpringerLink. Biocompatibility of Dental Materials: Springer Berlin Heidelberg; 2009. p. 99-105
8. Albers HF. Tooth colored restoratives : principles and techniques. 9th ed. ed. Hamilton: B.C. Decker; 2002. p. 82-90
9. Albers HF. Tooth colored restoratives : principles and techniques. 9th ed. ed. Hamilton: B.C. Decker; 2002. p. 135-141
10. De Munck J, Van Landuyt K, Peumans M, Poitevin A, Lambrechts P, Braem M, et al. A Critical Review of the Durability of Adhesion to Tooth Tissue: Methods and Results. Journal of Dental Research 2005. p. 118-132.
11. Peumans M, Kanumilli P, De Munck J, Van Landuyt K, Lambrechts P, Van Meerbeek B. Clinical effectiveness of contemporary adhesives: A systematic review of current clinical trials. Dental Materials. 2005;21(9):864-181.
12. Albers HF. Tooth colored restoratives : principles and techniques. 9th ed. ed. Hamilton: B.C. Decker; 2002. p. 46
13. Tannlegetidene. En av tre unge har tannregulering. Den norske tannlegeforenings tidende. 2006;116(2):135-136.

14. Kotrogianni M, Rahiotis C. Resin Composites in Orthodontic Bonding. A Clinical Guide. Journal of Dentistry and Oral Biology. 2017;2(7).
15. Blaschke U, Eismann K, Böhme A, Paschke A, Schüürmann G. Structural alerts for the excess toxicity of acrylates, methacrylates, and propiolates derived from their short-term and long-term bacterial toxicity. Chemical Research in Toxicology. 2012;25:170-180.
16. Ansteinsson V, Kopperud HB, Morisbak E, Samuelsen JT. Cell toxicity of methacrylate monomers-The role of glutathione adduct formation. Journal of Biomedical Materials Research. 2013.
17. Ferracane JL. Resin composite—State of the art. Dental Materials. 2011;27:29-38.
18. Ruyter IE, Oysaed H. Composites for use in posterior teeth: composition and conversion. Journal of biomedical materials research. 1987;21:11-23.
19. Costa S, Galvão M, Jacomassi D, Bernardi M, Hernandes A, Souza Rastelli A, et al. Continuous and gradual photo-activation methods: influence on degree of conversion and crosslink density of composite resins. An International Forum for Thermal Studies. 2011;103:219-227.
20. Michelsen VB, Kopperud HBM, Lygre GB, Björkman L, Jensen E, Kleven IS, et al. Detection and quantification of monomers in unstimulated whole saliva after treatment with resin‐based composite fillings in vivo. European Journal of Oral Sciences. 2012;120:89-95.
21. Polydorou O, Hellwig E, König A, Kümmerer K. Long-term release of monomers from modern dental-composite materials. European Journal of Oral Sciences. 2009;117:68-75.
22. Gerzina TM, Hume WR. Diffusion of monomers from bonding resin-resin composite combinations through dentine in vitro. Journal of Dentistry. 1996;24:125-8.
23. Rogalewicz R, Voelkel A, Kownacki I. Application of HS-SPME in the determination of potentially toxic organic compounds emitted from resin-based dental materials. Journal of Environmental Monitoring. 2006;8(3):377-383.
24. Marquardt W, Seiss M, Hickel R, Reichl FX. Volatile methacrylates in dental practices. The journal of adhesive dentistry. 2009;11(2):101-107.
25. Van Landuyt KL, Nawrot T, Geebelen B, De Munck J, Snauwaert J, Yoshihara K, et al. How much do resin-based dental materials release? A meta-analytical approach. Dental Materials. 2011;27(8):723-747.

26. Henriks-eckerman M-l, Alanko K, Jolanki R, Kerosuo H, Kanerva L. Exposure to airborne methacrylates and natural rubber latex allergens in dental clinics. Journal of Environmental Monitoring. 2001;3(3):302-5.
27. Hagberg S, Ljungkvist G, Andreasson H, Karlsson S, Barregård L. Exposure to Volatile Methacrylates in Dental Personnel. Journal of Occupational and Environmental Hygiene. 2005;2(6):302-306.
28. Helmis CG, Tzoutzas J, Flocas HA, Halios CH, Stathopoulou OI, Assimakopoulos VD, et al. Indoor air quality in a dentistry clinic. Science of the Total Environment. 2007;377(2):349-365.
29. Ansteinsson V, Solhaug A, Samuelsen JT, Holme JA, Dahl JE. DNA-damage, cell-cycle arrest and apoptosis induced in BEAS-2B cells by 2-hydroxyethyl methacrylate (HEMA). Mutation research. 2011;723(2):158.
30. Ho YC, Huang FM, Lee SS, Chang YC. The regulation of cytotoxicity and cyclooxygenase-2 expression by 2-hydroxy-ethyl methacrylate in human osteoblasts are related to intracellular glutathione levels. Internastional Endodontic Journal. 2014;47(8):784-790.
31. Morisbak E, Ansteinsson V, Samuelsen JT. Cell toxicity of 2-hydroxyethyl methacrylate (HEMA): the role of oxidative stress. European Journal of Oral Sciences. 2015;123(4):282-287.
32. Samuelsen JT, Holme JA, Becher R, Karlsson S, Morisbak E, Dahl JE. HEMA reduces cell proliferation and induces apoptosis in vitro. Dental Materials. 2008;24:134-140.
33. Samuelsen JT, Kopperud HM, Dragland JA, Dahl IS, Holme T, Christensen JE. Role of thiol-complex formation in 2-hydroxyethyl- methacrylate-induced toxicity in vitro. Journal of Biomedical Materials Research. 2011;96(2):395-401.
34. Krifka S, Petzel C, Hiller K-A, Frank E-M, Bosl C, Spagnuolo G, et al. Resin monomer-induced differential activation of MAP kinases and apoptosis in mouse macrophages and human pulp cells. Biomaterials. 2010;31(11):2964-2975.
35. Roberts DW. Structure-activity relationships for skin sensitisation potential of diacrylates and dimethacrylates. Contact Dermatitis. 1987;17(5):281-289.
36. Sandberg E, Bergenholtz G, Kahu H, Dahlgren U. Low HEMA conjugation induces high autoantibody titer in mice. Journal of Dental Research. 2005;84(6):537-541.

37. Helsedirektoratet. Nasjonale faglige retningslinjer for utredning og behandling ved mistanke om bivirkninger fra odontologiske biomaterialer. In: Helsedirektoratet avdeling omsorg og tannhelse; 2008.
38. Josephy PD, Mannervik B. Molecular toxicology. 2nd ed. ed. New York: Oxford University Press; 2006. p. 303-310
39. Bulleid NJ, Ellgaard L. Multiple ways to make disulfides. Trends in biochemical sciences. 2011;36(9):485-492.
40. Janssen-Heininger YM, Nolin JD, Hoffman SM, van der Velden JL, Tully JE, Lahue KG, et al. Emerging mechanisms of glutathione-dependent chemistry in biology and disease. Journal of cellular biochemistry. 2013;114(9):1962-1968.
41. Aquilano K, Baldelli S, Ciriolo MR. Glutathione: new roles in redox signaling for an old antioxidant. Frontiers in pharmacology. 2014;5:196.
42. Pompella A, Visvikis A, Paolicchi A, Tata VD, Casini AF. The changing faces of glutathione, a cellular protagonist. Biochemical pharmacology. 2003;66(8):1499-1503.
43. Anathy V, Roberson EC, Guala AS, Godburn KE, Budd RC, Janssen-Heininger YM. Redox-based regulation of apoptosis: S-glutathionylation as a regulatory mechanism to control cell death. Antioxidants & redox signaling. 2012;16(6):496-505.
44. Sies H, Jones D. Oxidative Stress. Elsevier. 2010. p. 45-48
45. Dalle-Donne I, Milzani A, Gagliano N, Colombo R, Giustarini D, Rossi R. Molecular mechanisms and potential clinical significance of S-glutathionylation. Antioxidants & redox signaling. 2008;10(3):445-473.
46. Jancova P, Anzenbacher P, Anzenbacherova E. Phase II drug metabolizing enzymes. Biomedical papers of the Medical Faculty of the University Palacky, Olomouc, Czechoslovakia. 2010;154(2):103-116.
47. Franklin MR. Phase II biotransformation reactions-glutathione-s-transferase. Elsevier. 2011. p. 1-8
48. Strachan T, Read AP. Human molecular genetics. 4th ed. ed. New York: Garland Science; 2011. p. 20-29
49. Lodish H. Molecular cell biology. 7th ed. ed. New York: Freeman; 2013. p. 35-37
50. Dalle-Donne I, Rossi R, Giustarini D, Colombo R, Milzani A. S-glutathionylation in protein redox regulation. Free Radical Biology and Medicine. 2007;43(6):883-898.

51. Dalle-Donne I, Rossi R, Colombo G, Giustarini D, Milzani A. Protein S-glutathionylation: a regulatory device from bacteria to humans. Trends in biochemical sciences. 2009;34(2):85-96.
52. Aesif SW, Janssen-Heininger YM, Reynaert NL. Protocols for the detection of s-glutathionylated and s-nitrosylated proteins in situ. Methods in enzymology. 2010;474:289-296.
53. Mieyal JJ, Chock PB. Posttranslational modification of cysteine in redox signaling and oxidative stress: Focus on s-glutathionylation. Antioxidants & redox signaling. 2012;16(6):471-475.
54. Xiong Y, Uys JD, Tew KD, Townsend DM. S-glutathionylation: from molecular mechanisms to health outcomes. Antioxidants & redox signaling. 2011;15:233-270.
55. Ribas V, Garcia-Ruiz C, Fernandez-Checa JC. Glutathione and mitochondria. Frontiers in pharmacology. 2014;5:151.
56. Dalle-Donne I, Rossi R, Giustarini D, Colombo R, Milzani A. Actin S-glutathionylation: evidence against a thiol-disulphide exchange mechanism. Free radical biology & medicine. 2003;35(10):1185-1193.
57. Lillig CH, Berndt C, Holmgren A. Glutaredoxin systems. BBA - General Subjects. 2008;1780(11):1304-1317.
58. Tew KD, Townsend DM. Redox platforms in cancer drug discovery and development. Current Opinion in Chemical Biology. 2011;15:156-161.
59. Blanchoin L, Boujemaa-Paterski R, Sykes C, Plastino J. Actin dynamics, architecture, and mechanics in cell motility. Physiological Reviews. 2014. p. 235-263.
60. Terman JR, Kashina A. Post-translational modification and regulation of actin.(Report). Current Opinion in Cell Biology. 2013;25:30.
61. Dalle-Donne I, Carini M, Vistoli G, Gamberoni L, Giustarini D, Colombo R, et al. Actin Cys374 as a nucleophilic target of alpha,beta-unsaturated aldehydes. Free radical biology & medicine. 2007;42(5):583-598.
62. Fletcher DA, Mullins RD. Cell mechanics and the cytoskeleton. Nature. 2010;463(7280):485-492.
63. Lodish H. Molecular cell biology. 7th ed. ed. New York: Freeman; 2013. p. 776-90
64. Wang J, Boja ES, Tan W, Tekle E, Fales HM, English S, et al. Reversible glutathionylation regulates actin polymerization in A431 cells. The Journal of biological chemistry. 2001;276(51):477-486.

65. Giustarini D, Rossi R, Milzani A, Colombo R, Dalle-Donne I. S-glutathionylation: from redox regulation of protein functions to human diseases. Journal of cellular and molecular medicine. 2004;8(2):201-212.
66. Johansson M, Lundberg M. Glutathionylation of beta-actin via a cysteinyl sulfenic acid intermediary. BMC biochemistry. 2007;8:26.
67. Dalle-Donne I, Giustarini D, Rossi R, Colombo R, Milzani A. Reversible S-glutathionylation of Cys 374 regulates actin filament formation by inducing structural changes in the actin molecule. Free Radical Biology and Medicine. 2003;34:23-32.
68. Fiaschi T, Cozzi G, Raugei G, Formigli L, Ramponi G, Chiarugi P. Redox regulation of beta-actin during integrin-mediated cell adhesion. The Journal of biological chemistry. 2006;281(32):22983-22991.
69. Sakai J, Li J, Subramanian KK, Mondal S, Bajrami B, Hattori H, et al. Reactive oxygen species-induced actin glutathionylation controls actin dynamics in neutrophils. Immunity. 2012;37(6):1037-1049.
70. Reddel RR, Ke Y, Gerwin BI, McMenamin MG, Lechner JF, Su RT, et al. Transformation of human bronchial epithelial cells by infection with SV40 or adenovirus-12 SV40 hybrid virus, or transfection via strontium phosphate coprecipitation with a plasmid containing SV40 early region genes. Cancer research. 1988;48(7):1904.
71. Drew R, Miners JO. The effects of buthionine sulphoximine (BSO) on glutathione depletion and xenobiotic biotransformation. Biochemical pharmacology. 1984;33(19):2989-2994.
72. European Union Law. Council Directive 98/24/EC of 7 April 1998 on the protection of the health and safety of workers from the risks related to chemical agents at work. 1998.
73. Mosmann T. Rapid colorimetric assay for cellular growth and survival: application to proliferation and cytotoxicity assays. Journal of immunological methods. 1983;65(1-2):55-63.
74. Sylvester PW. Optimization of the tetrazolium dye (MTT) colorimetric assay for cellular growth and viability. Methods in molecular biology (Clifton, NJ). 2011;716:157.
75. Standardization Organization for Standardization. ISO 10993-5, Biological evaluation of medical devices-Part : Test of in vitro cytotoxicity. Annex C, MTT cytotoxicity test. 2009.

76. Cotgreave IA, Moldéus P. Methodologies for the application of monobromobimane to the simultaneous analysis of soluble and protein thiol components of biological systems. Journal of Biochemical and Biophysical Methods. 1986;13(4):231-49.
77. Mahmood T, Yang P-C. Western blot: Technique, theory, and trouble shooting. North American Journal of Medical Sciences. 2012;4(9):429-434.
78. Gross JH. Mass Spectrometry: A Textbook. Berlin, Heidelberg: Springer Berlin Heidelberg: Berlin, Heidelberg; 2011. p. 2-6
79. Michelsen VB. Organic leachables from resinbased dental restorative : characterization by use of combined gas chromatographymass spectrometry. The University of Bergen; 2007.
80. Bouillaguet S, Wataha JC, Hanks CT, Ciucchi B, Holz J. In vitro cytotoxicity and dentin permeability of HEMA. Journal of Endodontics. 1996;22(5):244-248.
81. Andersson J, Dahlgren U. Effects on mouse immunity of long-term exposure in vivo to minute amounts of HEMA. European Journal of Oral Sciences. 2011;119(2):109-114.

9 Appendix

9.1 Equipment and software

Table 9-1: List of equipment and software used in this thesis.

Product	Producer
Adobe Illustrator CS5	Adobe system software, Ireland
Adobe Photoshop CS5	Adobe system software, Ireland
Centrifuge, Rotina 35R	Hettich Lab Technologies, Germany
ACD ChemSketch (freeware)	Advanced Chemistry Development Labs, Berkshire, UK
CO_2 incubator (SANYO MCO-18AIC(UV))	Surplus Solutions, LLC, USA
Electrophoresis systems and blotting module	Bio-Rad Laboratories, Inc., CA, USA
Flow Cytometer, Cell lab Quanta™ SC	Beckman Coulter, Florida, USA
GraphPad prism 7 software	GraphPad Sofware, CA, USA
Masshunter Qualitative analysis software B.07.00	Agilent Technologies, CA, USA
Microsoft Excel 2010	Microsoft corporation, USA
Mini-PROTEAN Tetra cell	Bio-Rad Laboratories, Inc., CA, USA
Mini-PROTEAN® Tetra handcast systems	Bio-Rad Laboratories, Inc., CA, USA
Mini Trans-Blot® cell	Bio-Rad Laboratories, Inc., CA, USA
Moxi Z, mini automated cell counter	ORFLO Technologies, USA
Multicycle software	Phoenics Flow Systems, CA, USA
Image Studio Software Version 5.2	LI-COR GmbH, Germany
Odyssey CLx Western blot Scanner	LI-COR GmbH, Germany
Olympus BX51 Fluorescence Microscope	Olympus, Germany
Olympus C7070 Camera	Olympus, Germany
Olympus DP80 Camera	Olympus, Germany
Olympus CKX41 Inverted Phase Contrast Microscope	Olympus, Germany
Olympus fluoview FV1200 Confocal Laser Scanning Microscope	Olympus, Germany
Pipettes	Thermo Scientific, USA
Pipette tips	VWR International GmbH, Darmstadt, Germany
PowerPack™ High-Current Power Supply	Bio-Rad Laboratories, Inc., CA, USA
ScanLaf biological safety cabinets class 2 - Mars	Labogene, Denmark
Sonics Vibra Cell ™ VCX 130	Sonics & Materials Inc., CT, USA
Spectrophotometric microtiter plate reader, Synergy H1 hybrid reader	BioTek Instruments Inc., USA
Sterile 6 and 12 sample well-plates	Costar Cornar Incorporated, USA
Sterile Cell dishes 21 cm^2	Costar Cornar Incorporated, USA
Sterile cell culture flask 75 cm^2	Falcon BD Biosciences, USA
Sterile fine pipettes	Thermo Scientific, USA
Sterile fine pipette tipps	VWR International GmbH, Darmstadt, Germany
UHPLC-QqQ-MS	Agilent Technologies, CA, USA

9.2 Reagents and chemicals

Table 9-2 a: List of reagents and chemicals used in this thesis.

Chemical compound	CAS	Product number	Manufacturer
β-actin (8H10D10) Mouse mAb	-	3700	Cell Signalling Technologies, USA
β-actin antibody	-	4967	Cell Signalling Technologies, USA
2- hydroxyethyl methacrylate	868-77-9	477028	Sigma-Aldrich, St. Louis, USA
2- mercaptoethanol (60-24-2)	60-24-2	M6250	Sigma-Aldrich, St. Louis, USA
30% Acrylamide/Bis Solutiom	79-06-1 (acrylamide) 110-26-9 (N,N'-methylenediacrylamide)	161-0158	Bio-Rad Laboratories, Inc., CA, USA
Acetonitril	75-05-8	270717	Sigma-Aldrich, St. Louis, USA
Alexa Fluor® 594 Goat anti-mouse	-	A11032	Life Technologies, CA, USA
Alexa Fluor® 488 Phalloidin	-	8878	Cell Signalling Technologies, USA
Ammonium acetat	631-61-8	A1542	Sigma-Aldrich, St. Louis, USA
Ammonium persulfate (APS)	7727-54-0	A3678	Sigma-Aldrich, St. Louis, USA
Anti-glutathione antibody	-	19534	Abcam, Cambridge, UK
BEAS-2B cell line	-	95102433	Sigma-Aldrich, St. Louis, USA
Bovine serum albumin	9048-46-8	A7906	Sigma-Aldrich, St. Louis, USA
Bromobimane (mBrB)	71418-44-5	69898	Sigma-Aldrich, St. Louis, USA
Bromophenol blue sodium salt	62625-28-9	B8026	Sigma-Aldrich, St. Louis, USA
Buthionine sulfoximine (BSO)	83730-53-4	B2515	Sigma-Aldrich, St. Louis, USA
Citrate Buffer (8.6% sucrose, 1.2% tri-sodium citrate, 5% DMSO in dH_2O)	-	-	Pre-made by NIOM
Dimethyl sulphoxide (DMSO)	67-68-5	116743	Merck KGaA, Darmstadt, Germany
Fetalt bovine serum (FBS)	-	F4135	Sigma-Aldrich, St. Louis, USA
Formic acid	64-18-6	5.43804	Sigma-Aldrich, St. Louis, USA
Glycerol	56-81-5	24387.292	VWR International GmbH, Darmstadt, Germany
Glycine	56-40-6	G7126	Sigma-Aldrich, St. Louis, USA
HEPES buffer saline solution	-	CC5024	Lonza, Verviers, Belgium
Hoechst 33342 (23491-52-3)	23491-52-3	B2261	Sigma-Aldrich, St. Louis, USA
IRDye® 680CW Goat Anti-Rabbit	-	926-68071	LI-COR GmbH, Germany
IRDye® 680CW Goat Anti-Mouse	-	926-32210	LI-COR GmbH, Germany
IRDye® 800CW Goat Anti-Rabbit	-	926-32211	LI-COR GmbH, Germany
LHC-9 medium	-	12680-013	Life Technologies, CA, USA
Methanol	67-56-1	106007	Merck KGaA, Darmstadt, Germany
Nuclear Isolations and staining solution (NIM-DAPI)	-	731085	NPE Systems, Florida, USA
Paraformaldehyde	30525-89-4	P6148	Sigma-Aldrich, St. Louis, USA
Phosphate buffered saline 1x (PBS)	-	BE12-702F	Lonza, Verviers, Belgium
Poncau S	6226-79-5	P-3504	Sigma-Aldrich, St. Louis, USA
PureCol, Bovine Collagen	-	5005	CellSystems Biotechnologi GmbH, Germany
ProLong®Gold Antifade reagent with DAPI	-	P36935	Life Technologies, CA, USA
Propidium iodide solution (PI)	25535-16-4	70335	Sigma-Aldrich, St. Louis, USA
Skim milk powder	-	70166	Sigma-Aldrich, St. Louis, USA
Sodium chloride	7647-14-5	S5886	Sigma-Aldrich, St. Louis, USA
Sodium dodecyl sulfate (SDS)	151-21-3	L4390	Sigma-Aldrich, St. Louis, USA
Sucrose	57-50-1	S8501	Sigma-Aldrich, St. Louis, USA

Table 9-2 b: List of reagents and chemicals used in this thesis.

Chemical compound	CAS	Product number	Manufacturer
Synthetic peptides	-	-	GenScript, USA
TEMED	110-18-9	T9281	Sigma-Aldrich, St. Louis, USA
Thiazolyl Blue Tetrazolium bromide (MTT solution)	298-93-1	M2128	Sigma-Aldrich, St. Louis, USA
Tricine	5704-04-1	T5816	Sigma-Aldrich, St. Louis, USA
Tri-sodium citrate	6132-04-3	106447	Merck KGaA, Darmstadt, Germany
Triton® X-100	9002-93-1	T8787	Sigma-Aldrich, St. Louis, USA
Trypsin/EDTA 10x	-	BE-02-007E	Lonza, Verviers, Belgia
Trizma® base (tris-base)	77-86-1	T1503	Sigma-Aldrich, St. Louis, USA
Tween 20	9005-64-5	822184	Merck KGaA, Darmstadt, Germany
Virkon®	-	1701BA0072	DuPont Company, Suffolk, USA
Watman nitrocellulose membrane filter, 0.45 µm 13mm	-	WHA7184007	Sigma-Aldrich, St. Louis, USA

9.3 Plate coating procedure

Table 9-3: Coating of 12- and 24-well plates, 21 cm^2 dishes and 75 cm^2 flasks used for culturing BEAS-2B cells. Coated with HEPES-buffer with 0.1% collagen for 2 hours at room temperature before aspired and stored at -20°C.

Well, flask or dish	Reagent (HEPES-buffer with 0.1% collagen)
75 cm^2 flask	5 mL/flask
21 cm^2 dish	2 mL/dish
12-well plate	1 mL/well
24-well plate	0.5 mL/well

9.4 Recipe for reagents and gels used in SDS-PAGE and western blotting

Table 9-4: Recipe for reagents used in SDS-PAGE and western blotting analysis.

Reagent	Total volume	Recipe
10% APS	1 mL	0.1 g APS, dH_2O to final volume
10% SDS	100 mL	10 g SDS, dH_2O to final volume
Running buffer, pH 8.3	1000 mL	3.03 g Tris-base, 14.41 g Glycine, 1 g SDS, dH_2O to final volume, adjust pH
Sample buffer, pH 7	100 mL	12 g SDS, 1.817 g Tris-base, 30 g Glycerol, dH_2O to final volume, adjust pH
TBS-T, pH 7.5	1000 mL	6.06 g Tris-base, 8.76 g NaCl, 1 mL Tween 20, dH_2O to final volume, adjust pH
Transfer buffer	2000 mL	6.06 g Tris-base, 28.82 g Glycine,400 mL Methanol, dH_2O to final volume
Tris 0.5 M, pH 6.8	100 mL	6.06 g Tris-base, dH_2O to final volume, adjust pH
Tris 1.5 M , pH 8.8	100 mL	18.2 g Tris-base, dH_2O to final volume, adjust pH

Table 9-5: Recipe for 4 x 10% SDS-PAGE separation gel and stacking gel.

Reagent	Separation gel	Stacking gel
30% acrylamide/bis solution	10 mL	2.6 mL
Tris 1.5 M , pH 8.8	7.5 mL	-
Tris 0.5 M, pH 6.8	-	5 mL
dH_2O	11.9 mL	12.2 mL
10% SDS	300 µL	200 µL
10% APS	300 µL	100 µL
TEMED	12 µL	20 µL

9.5 Antibody dilution used in western blotting

Table 9-6: Dilution of primary antibodies used in western blotting.

Antibody	Dilution
β-actin	1:2500
Anti-glutathione	1:1000
IRDye® 680CW Goat anti-rabbit	1:5000
IRDye® 680CW Goat anti-mouse	1:5000
IRDye® 800CW Goat anti-rabbit	1:5000

9.6 Antibody dilution used in Immunofluorescence

Table 9-7: Dilution of primary antibodies used in immunofluorescence.

Antibody	Dilution
β-actin	1:600
Anti-glutathione	1:150
Alexa fluor®488 Phalloidin	1:20
Alexa Fluor®594 Goat anti-mouse	1:400